Efficient and Stereo-selective Synthesis of Monomeric and Bi-metallic Pincer Complexes Containing Pd-bonded Stereogenic Carbons

Wee Shan Tay, Xiang-Yuan Yang, Yongxin Li, Sumod A. Pullarkat, Pak-Hing Leung*

Division of Chemistry & Biological Chemistry, School of Physical and Mathematical Sciences, Nanyang Technological University, Singapore 637371, Singapore Fax: (+65) 6791 1961; e-mail: pakhing@ntu.edu.sg.

Supporting Information

Table of Contents **S1**

General Information

All reactions were carried out under a positive pressure of nitrogen using standard Schlenk techniques. NMR spectra were recorded on Bruker AV 300, AV 400 and AV 500 spectrometers. Chemical shifts were reported in ppm and referenced to an internal $SiMe_4$ standard (0 ppm) for ^1H NMR, chloroform-d (77.23 ppm) for ^{13}C NMR, and an external 85% H_3PO_4 for $^{31}P\{^1H\}$ NMR. DCM, DCE, DEE, toluene, acetone, acetonitrile and MeOH were purchased from their respective companies and used as supplied. THF was distilled prior to use. Solvents were degassed when necessary. A Low Temp Pairstirrer PSL-1400 was used for controlling low temperature reactions. Column chromatography was carried out with Silica gel 60 (Merck). Melting points were measured using SRS Optimelt Automated Point System SRS MPA100. Optical rotation were measured with JASCO P-1030 Polarimeter in the specified solvent in a 0.1 dm cell at 22.0°C.

The palladacycle (S)-**2**[1], enones **1**,[2] **5**[3] and **11**,[4] PC(sp^2)P PdCl complex (*R*,*R*)-**7**[3] were prepared according to literature methods. $PdCl_2(NCMe)_2$ was prepared by adding $PdCl_2$ portionwise to boiling acetonitrile under vigorous stirring for 30 mins. The yellow suspension was filtered and the yellow residue ($PdCl_2(NCMe)_2$) washed with acetonitrile and dried. All other reactants and reagents were used as supplied.

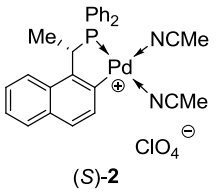

(*S*)-**2**

Figure s1. Palladacycle catalyst involved in this work.

Caution! *Perchlorate salts of metal complexes are potentially explosive compounds and should be handled with care.*

Synthesis of dienone 14[5]

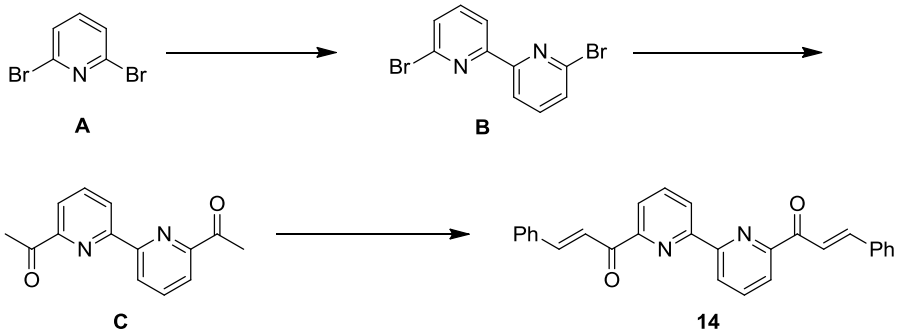

Scheme s1. Synthesis of dienone **14**.

A solution of 2,6-dibromopyridine **A** (10.0 g, 42.2 mmol, 1.0 equiv.) in DEE (150 mL) at 0°C was treated with 2.5 M *n*-BuLi in DEE (16.9 mL, 42.3 mmol, 1.0 equiv.) and stirred for 1 h. Anhydrous $CuCl_2$ (2.84 g, 21.1 mmol, 0,5 equiv.) was added portionwise and the temperature maintained at -50°C for 30 min. The brown suspension was bubbled with O_2 until the mixture

turned green. The reaction mixture was allowed to warm up to room temperature, hydrolyzed with 6 N HCl (15 mL), solvent removed under reduced pressure and filtered. The residue was washed with dilute HCl (to remove traces of Cu), dissolved in EA, wash with water (2 X 50 mL), dry over $MgSO_4$, filtered and solvent removed. The crude product was recrystallized from benzene to afford white needles of **B**. Yield: 8.75 g, 27.9 mmol, 66%. Mp: 225-226°C. ^{1}H NMR ($CDCl_3$, 400 MHz): δ 8.38 (d, 2H, ^3J = 7.7 Hz, BrCNCC*H*), 7.67 (t, 2H, ^3J = 7.8 Hz, BrCCHC*H*), 7.50 (d, 2H, ^3J = 7.8 Hz, BrCC*H*). ^{13}C NMR ($CDCl_3$, 100 MHz): δ 155.8 (2C, BrCN*C*), 141.8 (2C, Br*C*), 139.5 (2C, BrCCH*C*H), 128.8 (2C, BrC*C*H), 120.4 (2C, BrCNC*C*H). Anal. Calcd for $C_{10}H_6Br_2N_2$: C, 38.25; H, 1.93; N, 8.92. Found: C, 38.58; H, 2.15; N, 9.19%. HRMS (+ESI) m/z: $(M + H)^+$ calcd for $C_{10}H_7Br_2N_2$, 312.8976; found, 312.8978.

To a solution of 6,6'-dibromo-2,2'-bipyridine **B** (3.50 g, 11.1 mmol, 1.0 equiv.) in THF (250 mL) at -80°C was added 2.5 M *n*-BuLi in DEE (9.36 mL, 23.4 mmol, 2.1 equiv.) and stirred for 1 h. *N*,*N*-dimethylacetamide (2.28 mL, 24.5 mmol, 2.2 equiv.) in DEE (50 mL) was added dropwise and the purple solution stirred for 2h. The mixture was raised to -10°C, hydrolyzed with 6 N HCl (20 mL), concentrated under reduced pressure and neutralized with dilute aq. NaOH. The organic layer was extracted with DCM (3 X 50 mL), washed with H_2O (2 X 50 mL), dried over $MgSO_4$, filtered and the solvent evaporated. The crude product was recrystallized from EtOH twice to afford pure **C**. Yield: 1.87 g, 7.80 mmol, 70%. Mp: 175-177°C. ^{1}H NMR ($CDCl_3$, 300 MHz): δ 8.72 (d, 2H, ^3J = 7.6 Hz, O=CCNCC*H*), 8.09 (d, 2H, ^3J = 7.6 Hz, O=CCC*H*), 8.00 (t, 2H, ^3J = 7.7 Hz, O=CCCHC*H*), 2.84 (s, 6H, CH_3). ^{13}C NMR ($CDCl_3$, 100 MHz): δ 200.2 (2C, *C*=O), 154.8 (2C, O=CCN*C*), 153.2 (2C, O=C*C*N), 138.1 (2C,O=CCCH*C*), 124.5 (2C, O=CCNC*C*H), 122.0 (2C, O=CC*C*H_2), 25.9 (2C, *C*H_3). Anal. Calcd for $C_{14}H_{12}N_2O_2$: C, 69.99; H, 5.03; N, 11.66. Found: C, 69.84; H, 5.40; N, 11.30%. HRMS (+ESI) m/z: $(M + H)^+$ calcd for $C_{14}H_{13}N_2O_2$, 241.0977; found, 241.0976.

A mixture of 1,1'-([2,2'-bipyridine]-6,6'-diyl)diethanone **C** (1.00 g, 4.16 mmol, 1.0 equiv.), benzaldehyde (0.93 mL, 9.16 mmol, 2.2 equiv.) and KOH (10 % w/v in MeOH, 20 mL) was refluxed overnight. The pure dienone **14** was crystallized from the reaction mixture. Yield: 1.30 g, 3.12 mmol, 75%. Mp: 251-252°C. ^{1}H NMR ($CDCl_3$, 400 MHz): δ 8.82 (d, 2H, ^3J = 7.7 Hz, O=CCNCC*H*), 8.46 (d, 2H, ^3J = 16.0 Hz, PhCH=C*H*), 8.29 (d, 2H, ^3J = 7.6 Hz, O=CCC*H*), 8.12 (t, 2H, ^3J = 7.8 Hz, O=CCCHC*H*), 8.02 (d, 2H, ^3J = 16.1 Hz, PhC*H*=CH), 7.78-7.77 (m, 4H, Ar), 7.48-7.46 (m, 6H, Ar). ^{13}C NMR ($CDCl_3$, 75 MHz): δ 189.5 (2C, *C*=O), 154.9 (2C, O=CCN*C*), 154.0 (2C, O=C*C*N), 145.1 (2C, Ph*C*H=CH), 138.4 (2C, O=CCCH*C*H), 135.5 (2C, Ph), 130.9 (2C, O=CCNC*C*H), 129.2 (4C, Ph), 129.0 (4C, Ph), 124.5 (2C, Ph), 123.5 (2C, PhCH=*C*H), 121.1 (s, 2C, O=CC*C*H). Anal. Calcd for $C_{28}H_{20}N_2O_2$: C, 80.75; H, 4.84; N, 6.73. Found: C, 81.01; H, 5.09; N, 6.50%. HRMS (+ESI) m/z: $(M + H)^+$ calcd for $C_{28}H_{21}N_2O_2$, 417.1603; found, 417.1604.

General procedure for the asymmetric hydrophosphination of compound 17.

A Schlenk tube was charged with $HPPh_2$ (12.1 mg, 65.0 μmol, 1.5 equiv), NCE (E = O, S) complex (2.2 μmol, 5 mol% for mono-metallic complex; 1.1 μmol, 2.5 mol% for bi-metallic complex), KOAc (0.86 μg, 8.7 μmol, 20 mol%), malonate **17** (10.7 μL, 43.3 μmol, 1.0

equiv.), solvent (3 mL) and stirred at RT for 24h. Subsequently, aq. H_2O_2 (31% w/w, 0.1 mL) was introduced to the mixture. The volatiles were removed and the crude product loaded directly onto silica gel column (1 *n*-hexane : 2 EA) to afford pure white solid(s) of **18a** (1,4-adduct) and/or **18b** (1,6-adduct). The data obtained for both products are consistent with literature.[6]

Reference

[1] Huang, Y.; Chew, R. J.; Li, Y.; Pullarkat, S. A.; Leung, P. H. *Org. Lett.* **2011**, *13*, 5862-5865.

[2] Singh P. K.; Singh, V. K. *Org. Lett.* **2008**, *10*, 4121-4124.

[3] Yang X.-Y.; Tay, W. S.; Li, Y.; Pullarkat, S. A.; Leung, P.-H. *Organometallics* **2015**, *34*, 1582-1588.

[4] Higuchi, M.; Otsuka, Y.; Shomura, R.; Kurth, D. G. *Thin Solid Films* **2008**, *516*, 2416-2420.

[5] Chotalia, R.; Constable, E. C.; Neuburger, M.; Smith, D. R.; Zehnder, M. *J. Chem. Soc., Dalton Trans.* **1996**, 4207-4216.

[6] Yang, X.-Y.; Gan, J. H.; Li, Y.; Pullarkat, S. A.; Leung, P.-H. *Dalton Trans.* **2015**, *44*, 1258-1263.

NMR Spectra

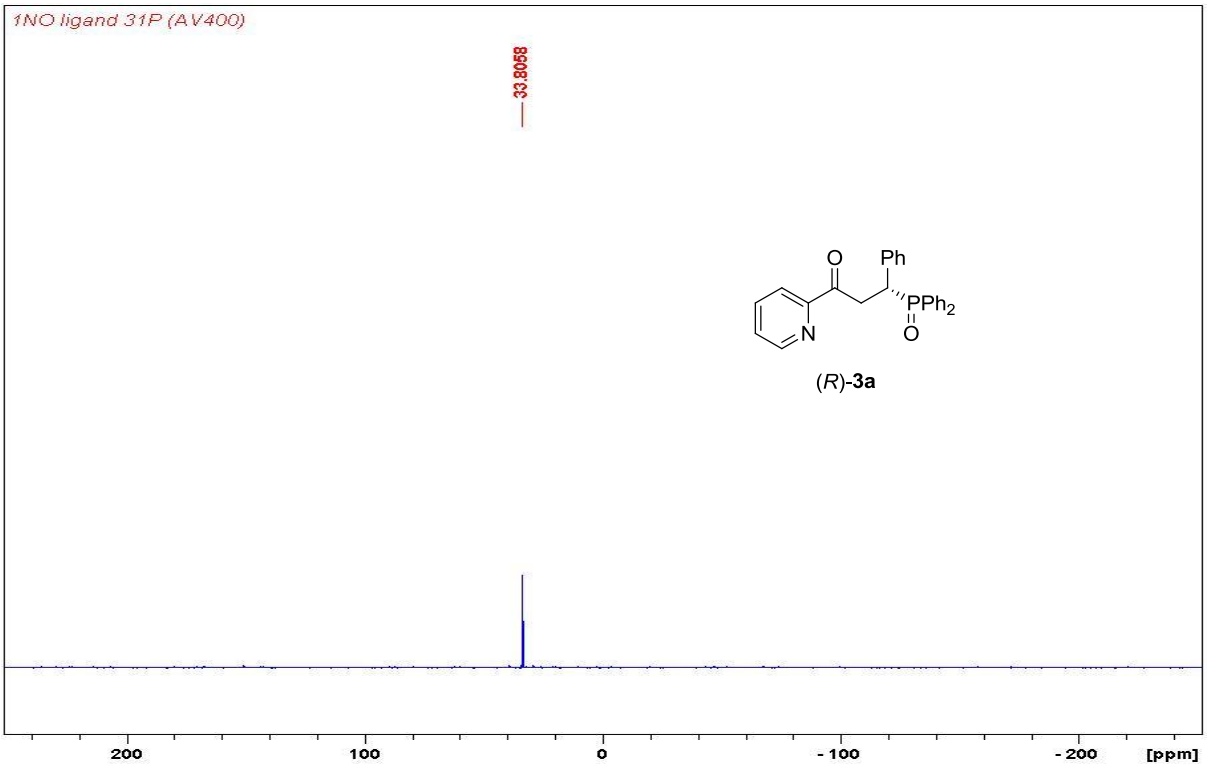

Figure s2. $^{31}P\{^{1}H\}$ NMR spectrum of compound (*R*)-**3a**.

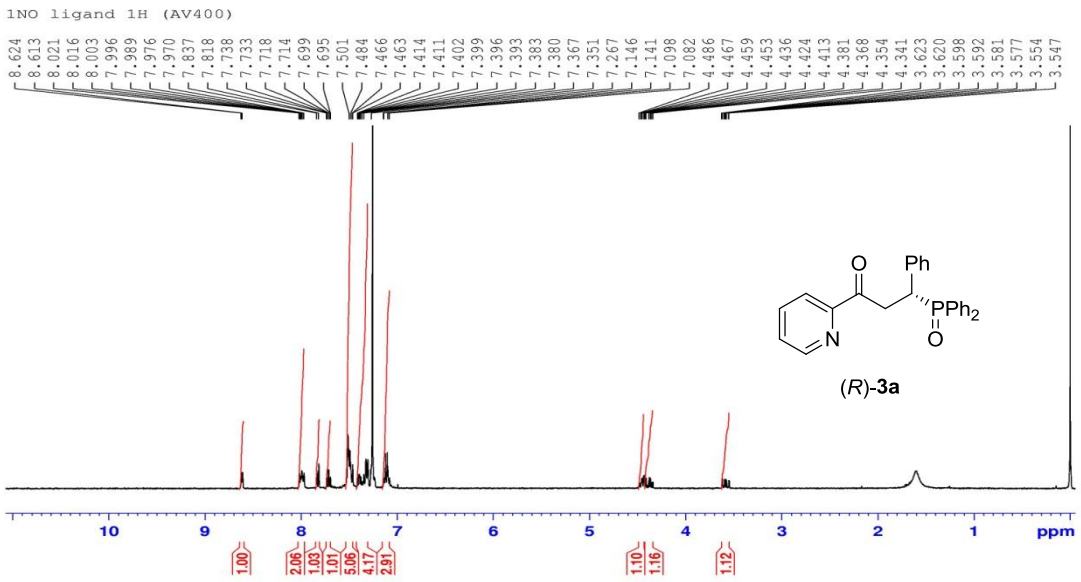

Figure s3. ^{1}H NMR spectrum of compound (*R*)-**3a**.

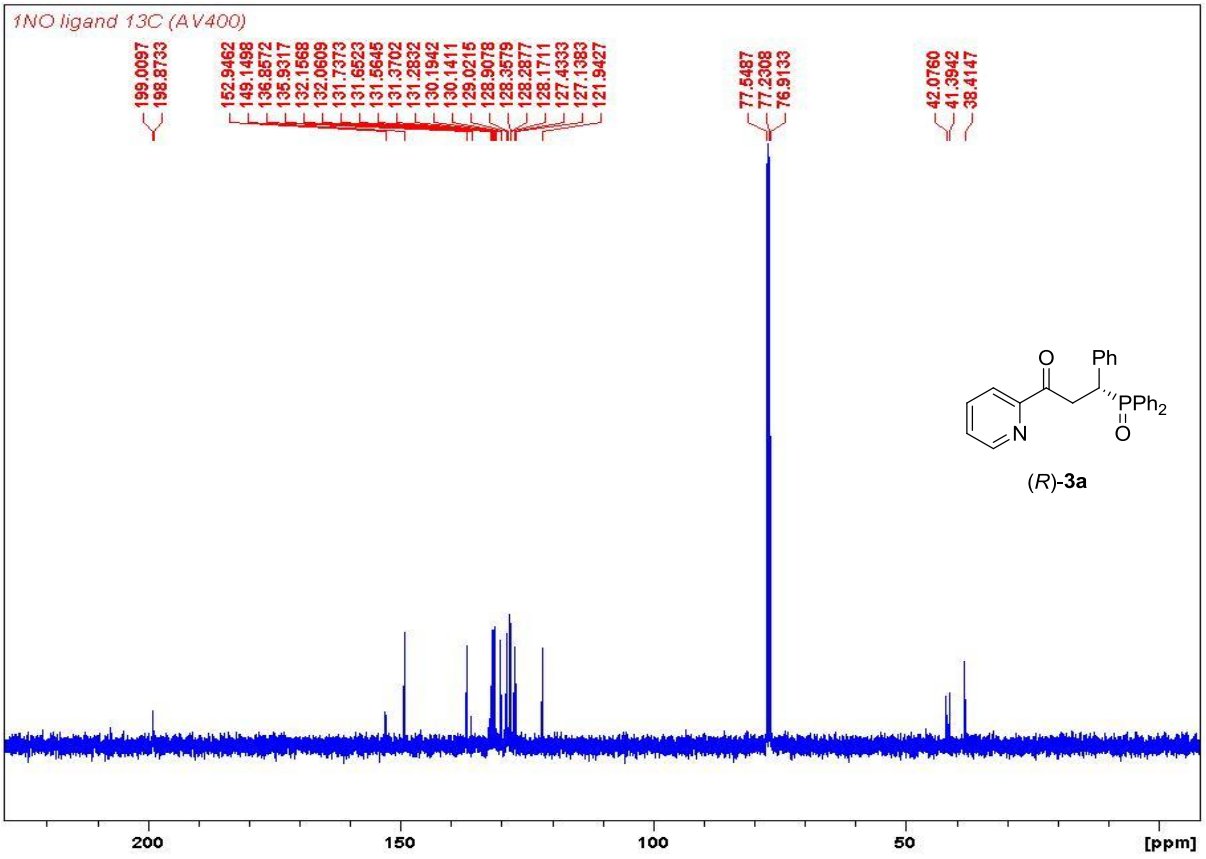

Figure s4. ^{13}C NMR spectrum of compound (*R*)-**3a**.

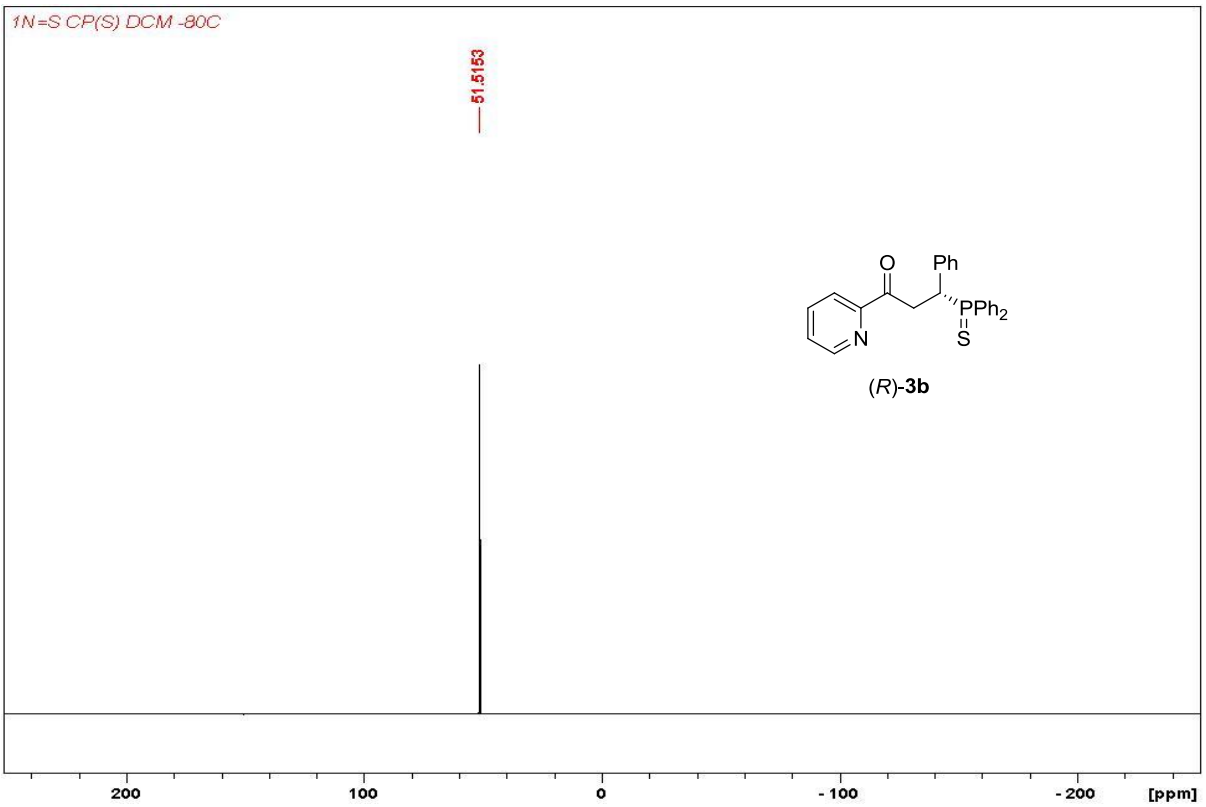

Figure s5. $^{31}P\{^{1}H\}$ NMR spectrum of compound (*R*)-**3b**.

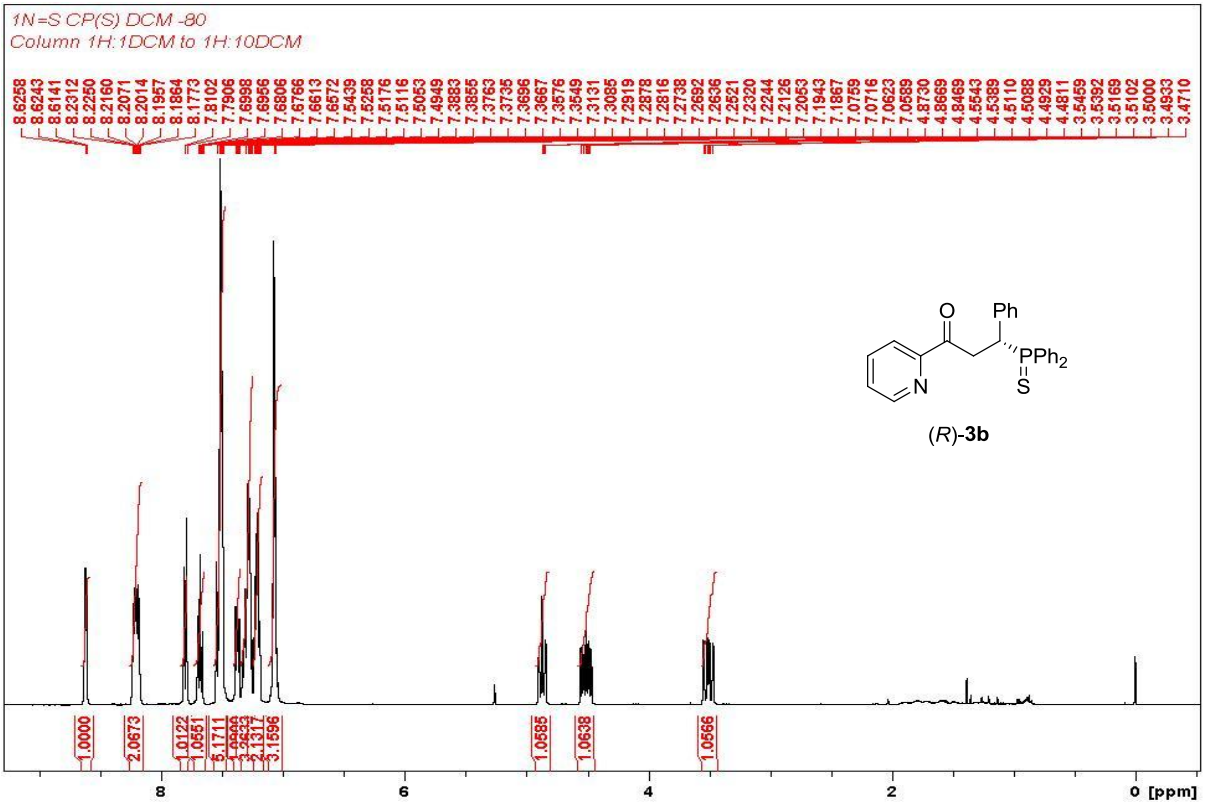

Figure s6. ^{1}H NMR spectrum of compound (*R*)-**3b**.

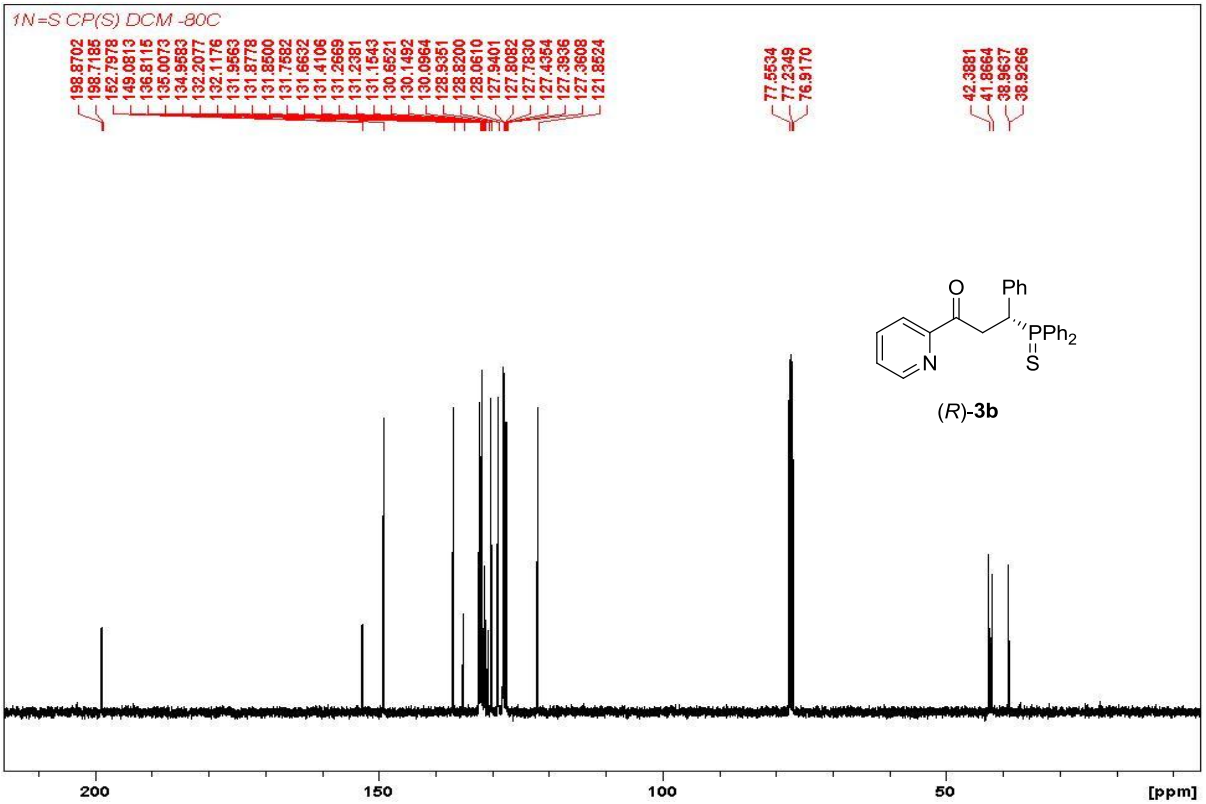

Figure s7. ^{13}C NMR spectrum of compound (*R*)-**3b**.

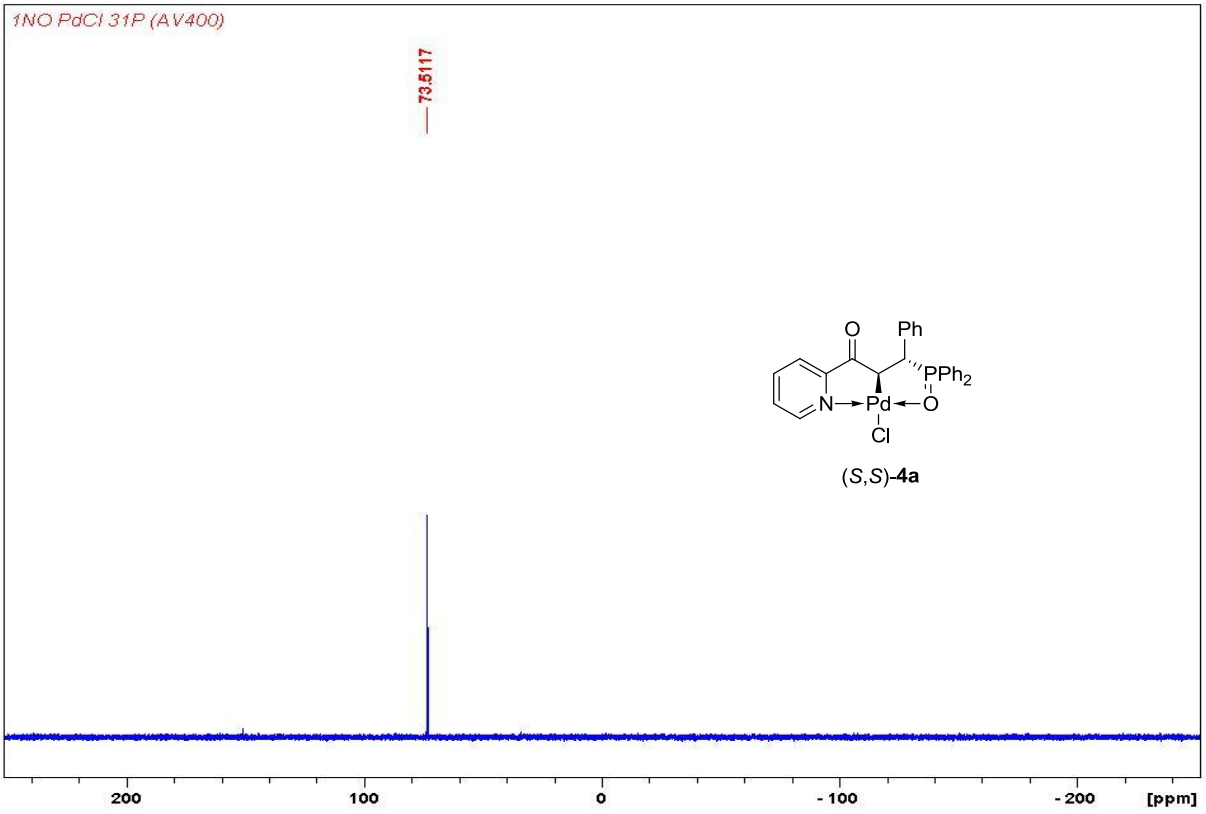

Figure s8. $^{31}P\{^{1}H\}$ NMR spectrum of compound (*S*,*S*)-**4a**.

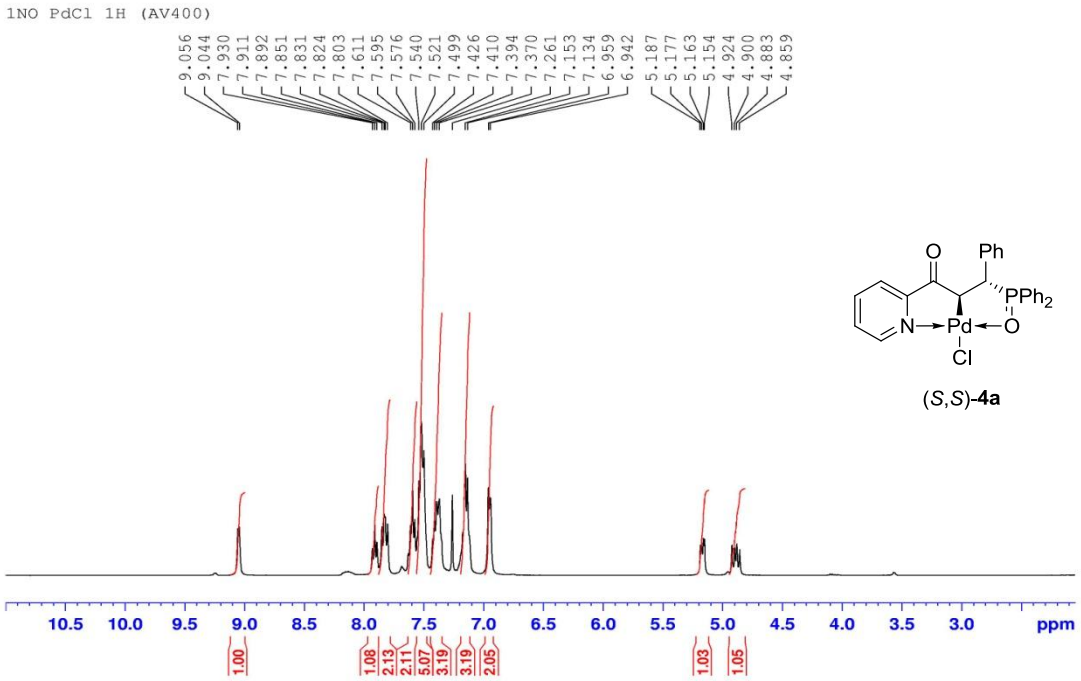

Figure s9. ^{1}H NMR spectrum of compound (*S*,*S*)-**4a**.

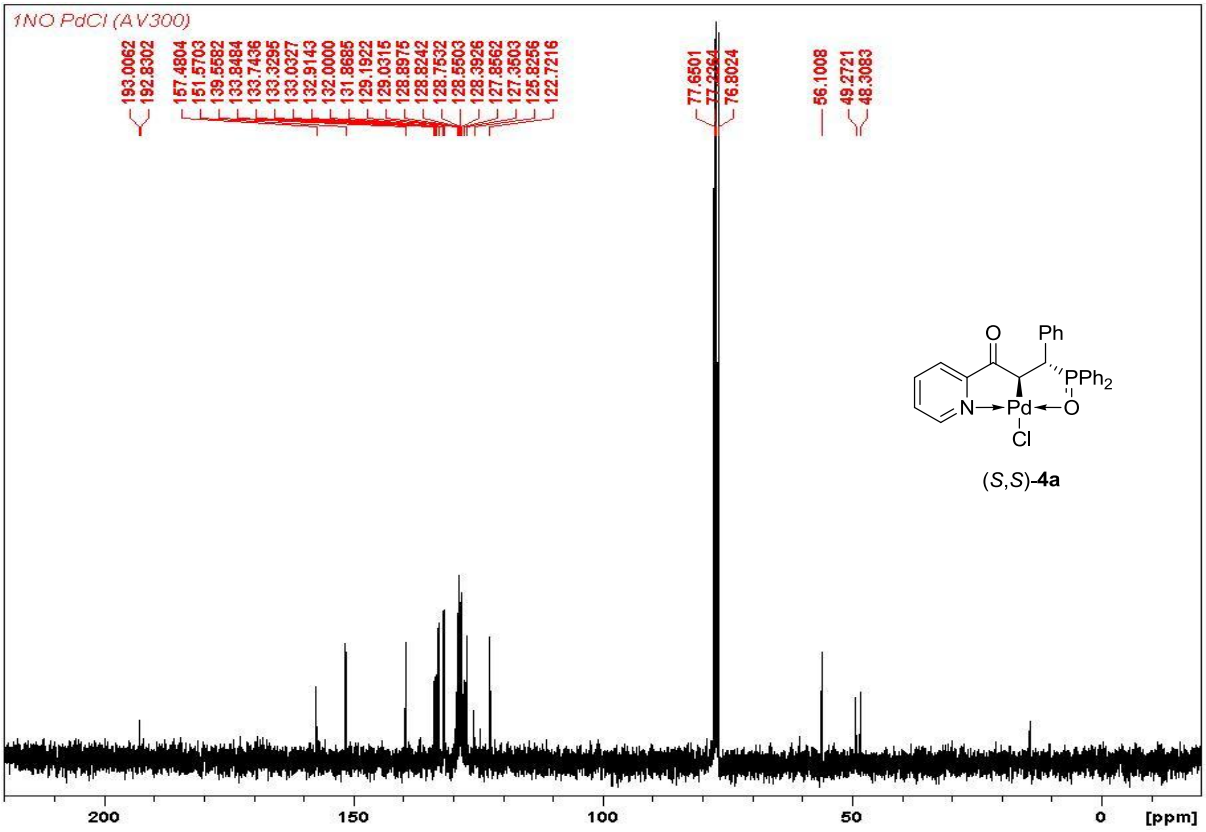

Figure s10. ^{13}C NMR spectrum of compound (*S*,*S*)-**4a**.

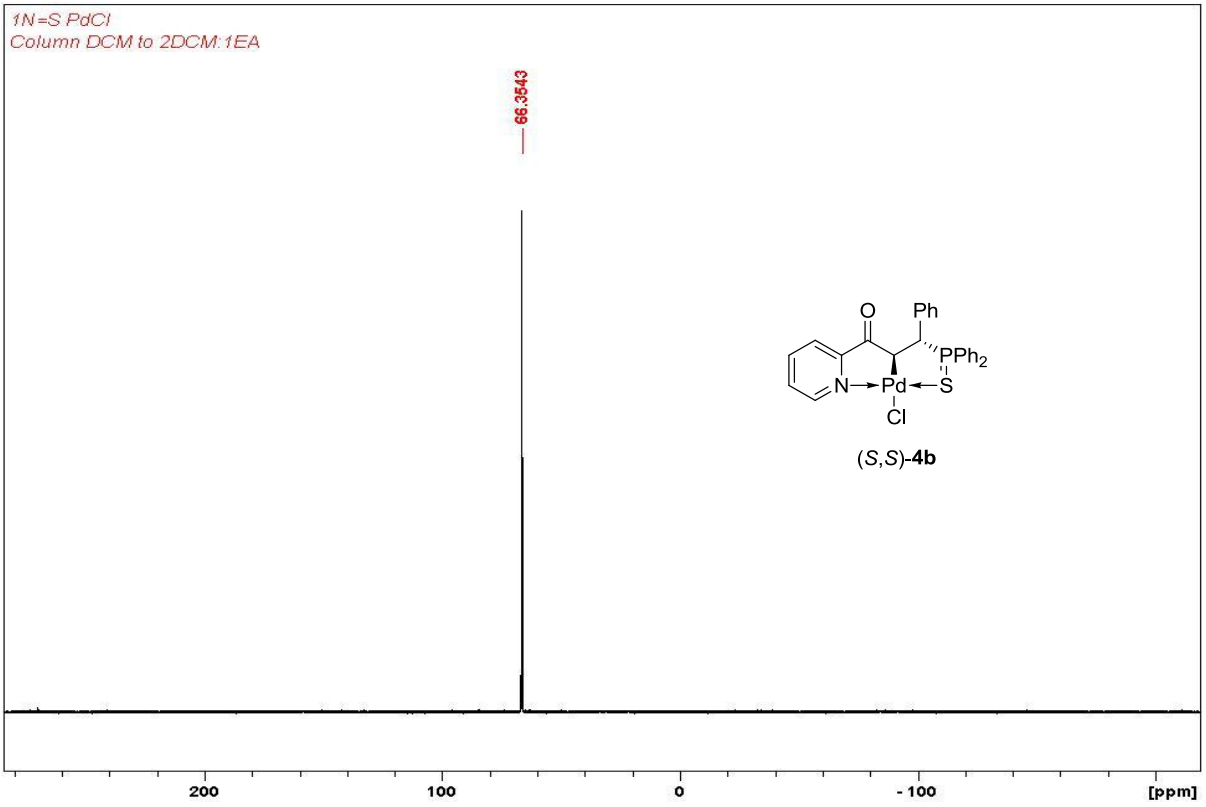

Figure s11. $^{31}P\{^{1}H\}$ NMR spectrum of compound (*S*,*S*)-**4b**.

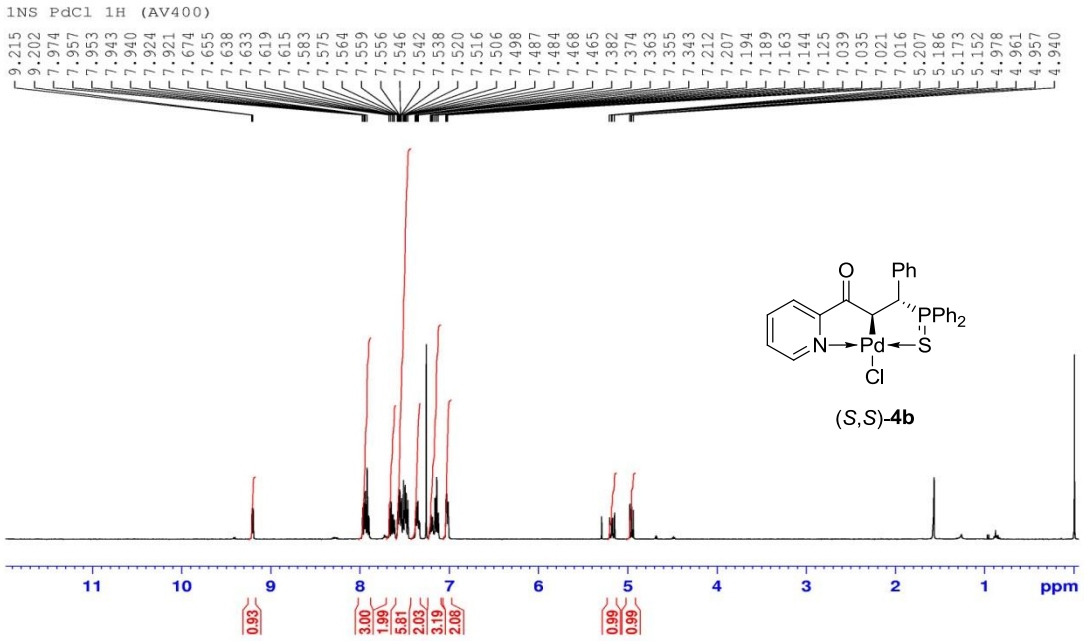

Figure s12. ^{1}H NMR spectrum of compound (*S*,*S*)-**4b**.

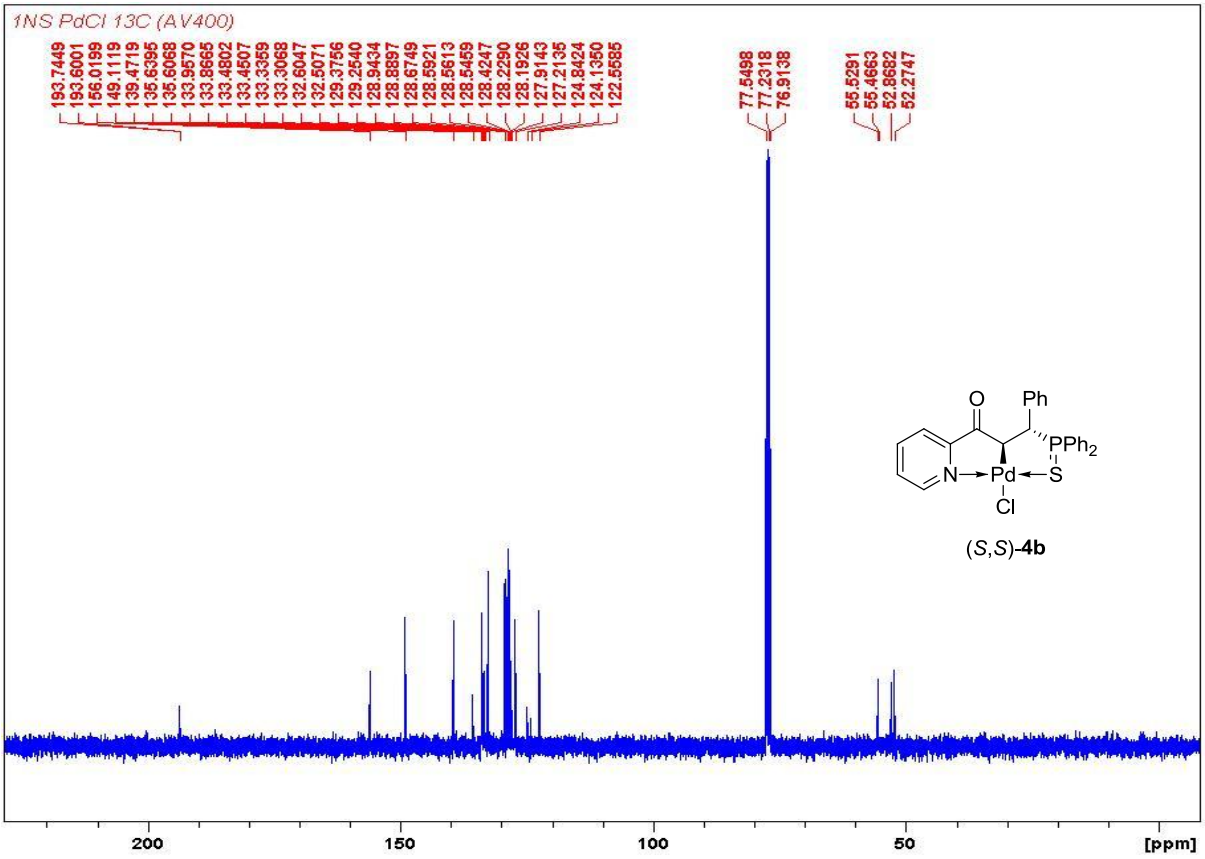

Figure s13. ^{13}C NMR spectrum of compound (*S*,*S*)-**4b**.

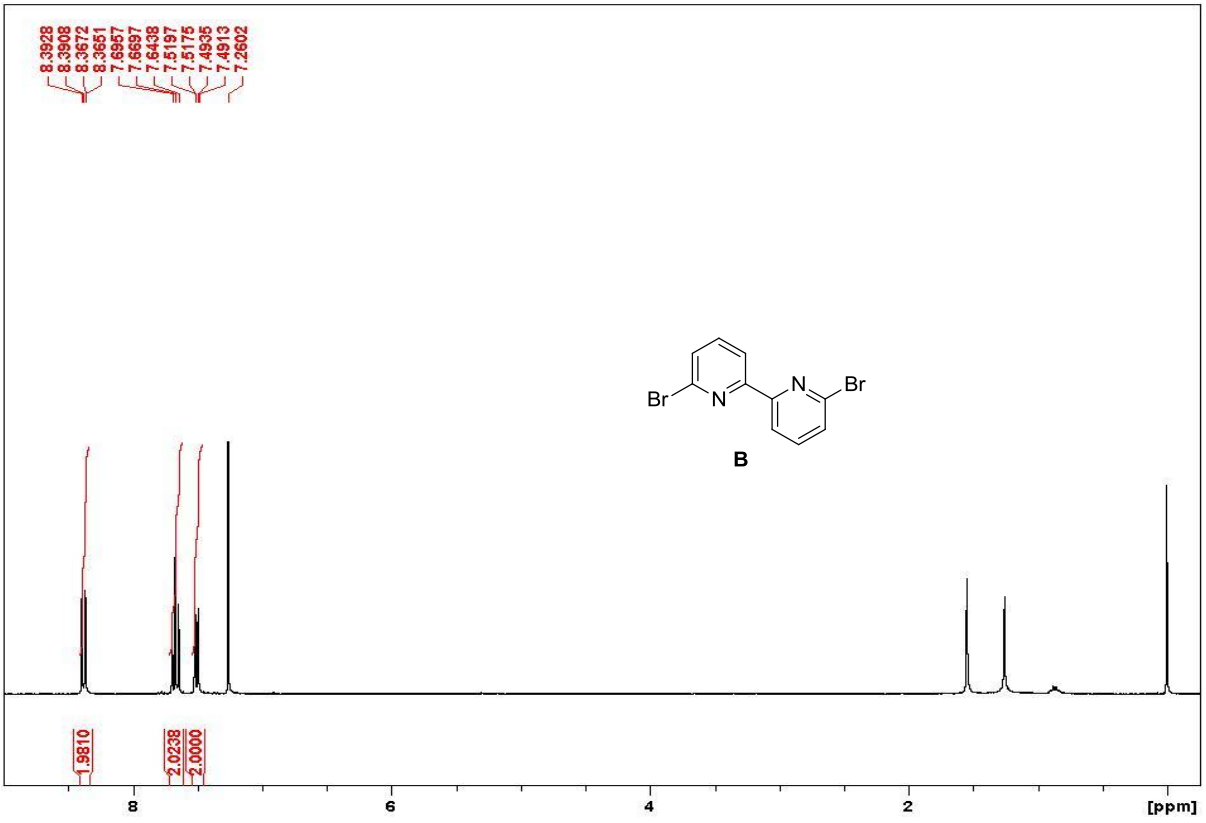

Figure s14. [1]H NMR spectrum of 6,6'-dibromo-2,2'-bipyridine **B**.

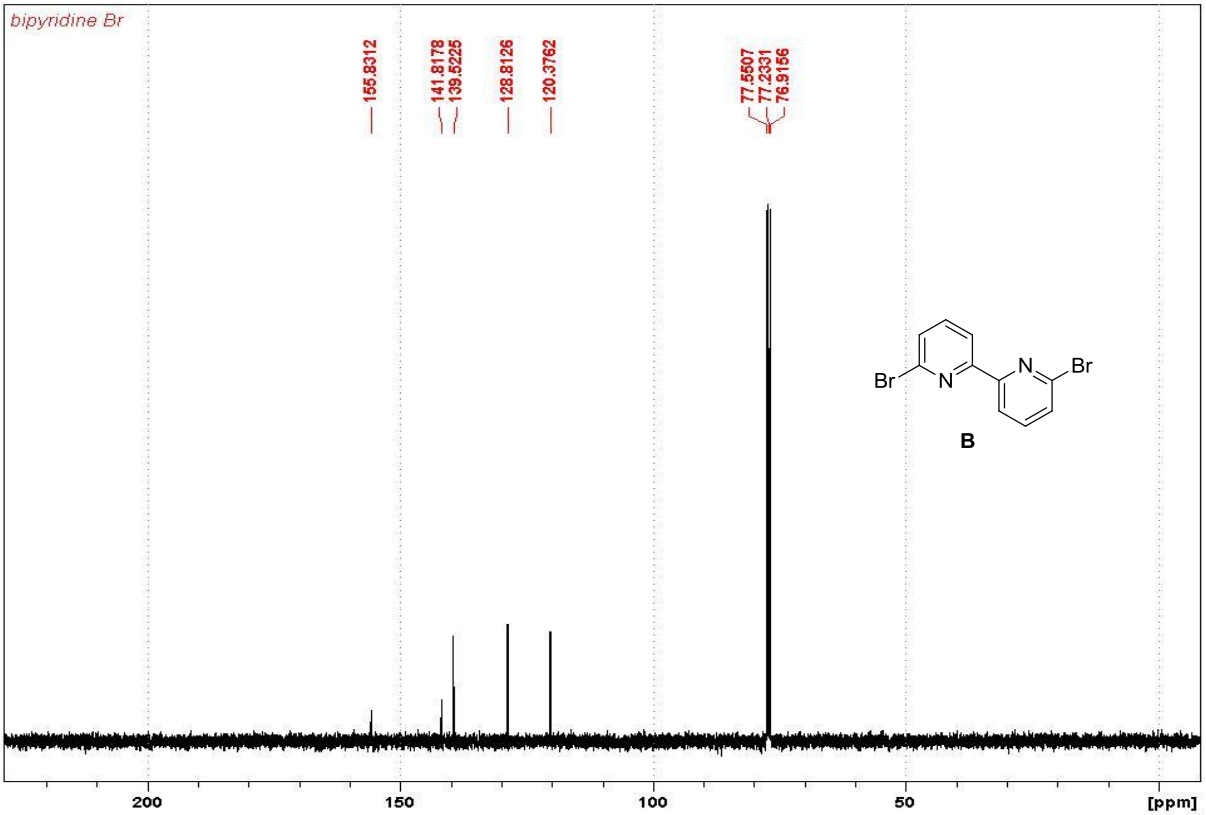

Figure s15. [13]C NMR spectrum of 6,6'-dibromo-2,2'-bipyridine **B**.

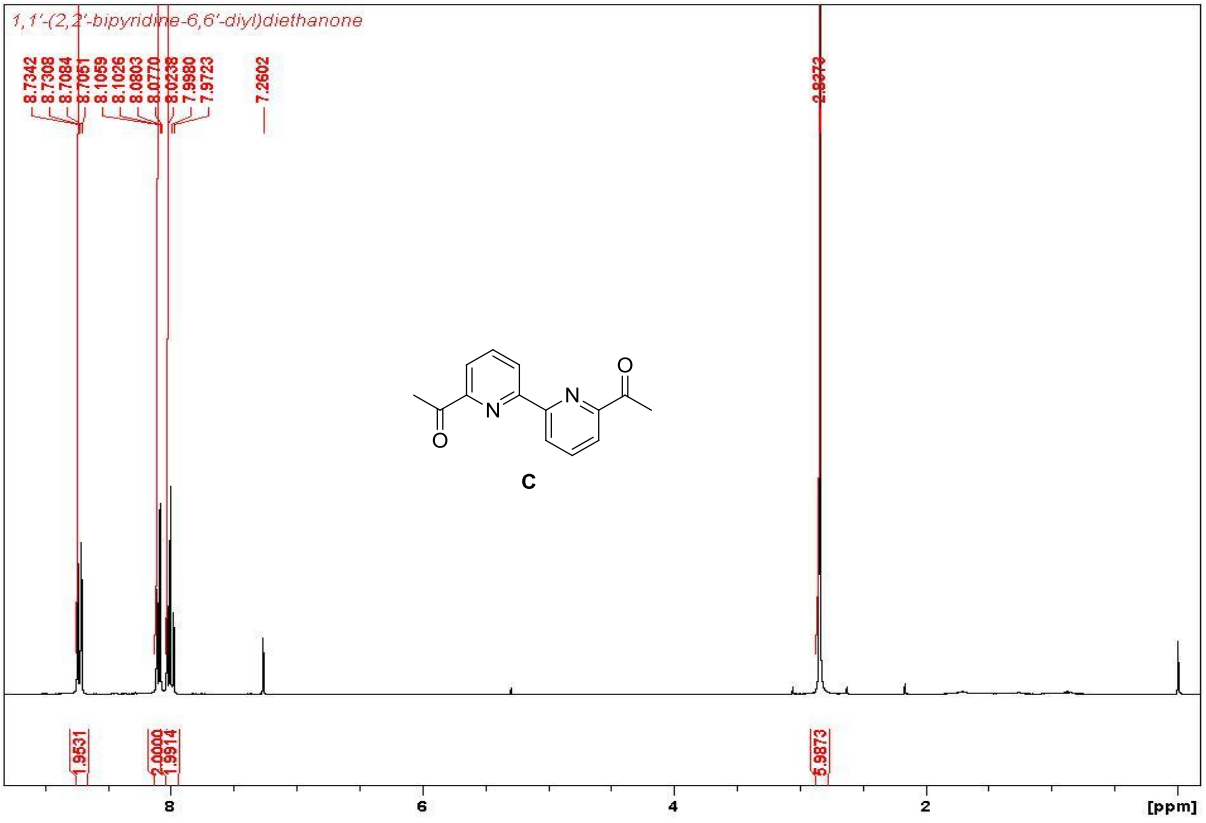

Figure s16. [1]H NMR spectrum of 1,1'-([2,2'-bipyridine]-6,6'-diyl)diethanone **C**.

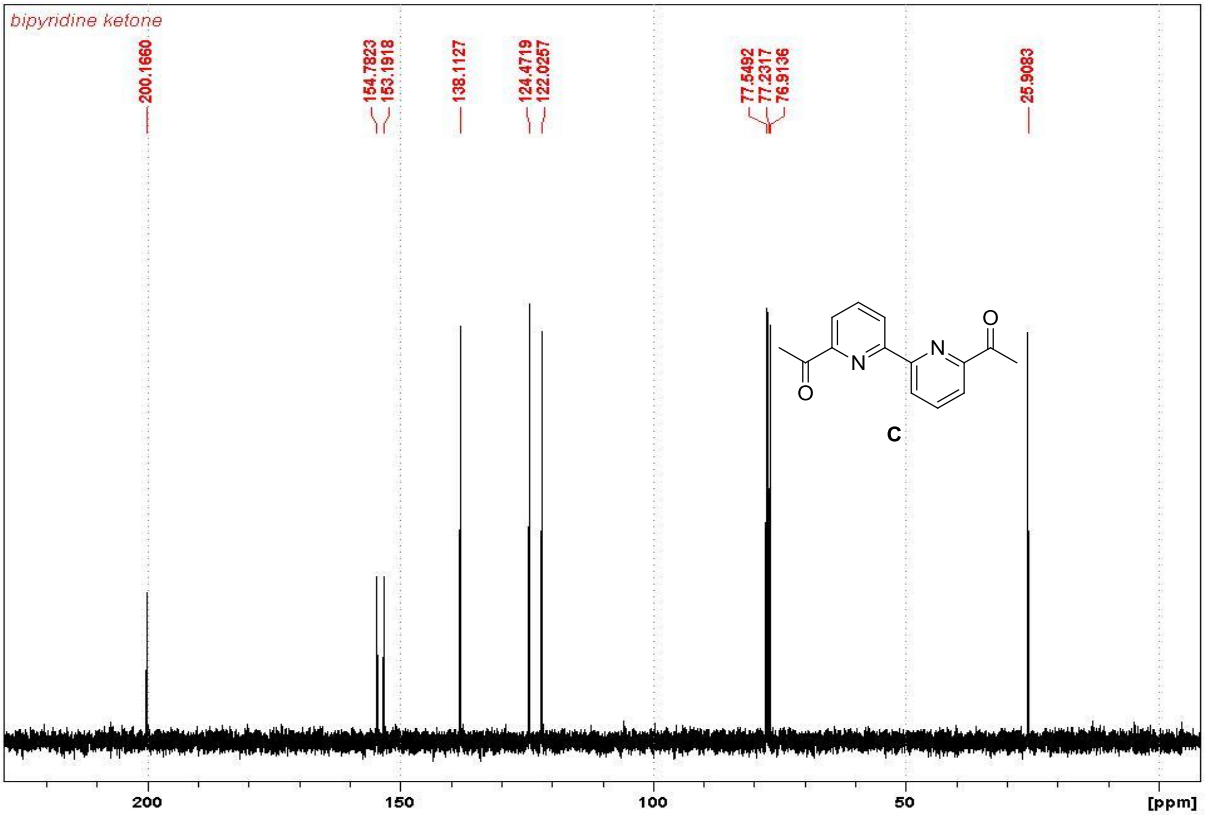

Figure s17. [13]C NMR spectrum of 1,1'-([2,2'-bipyridine]-6,6'-diyl)diethanone **C**.

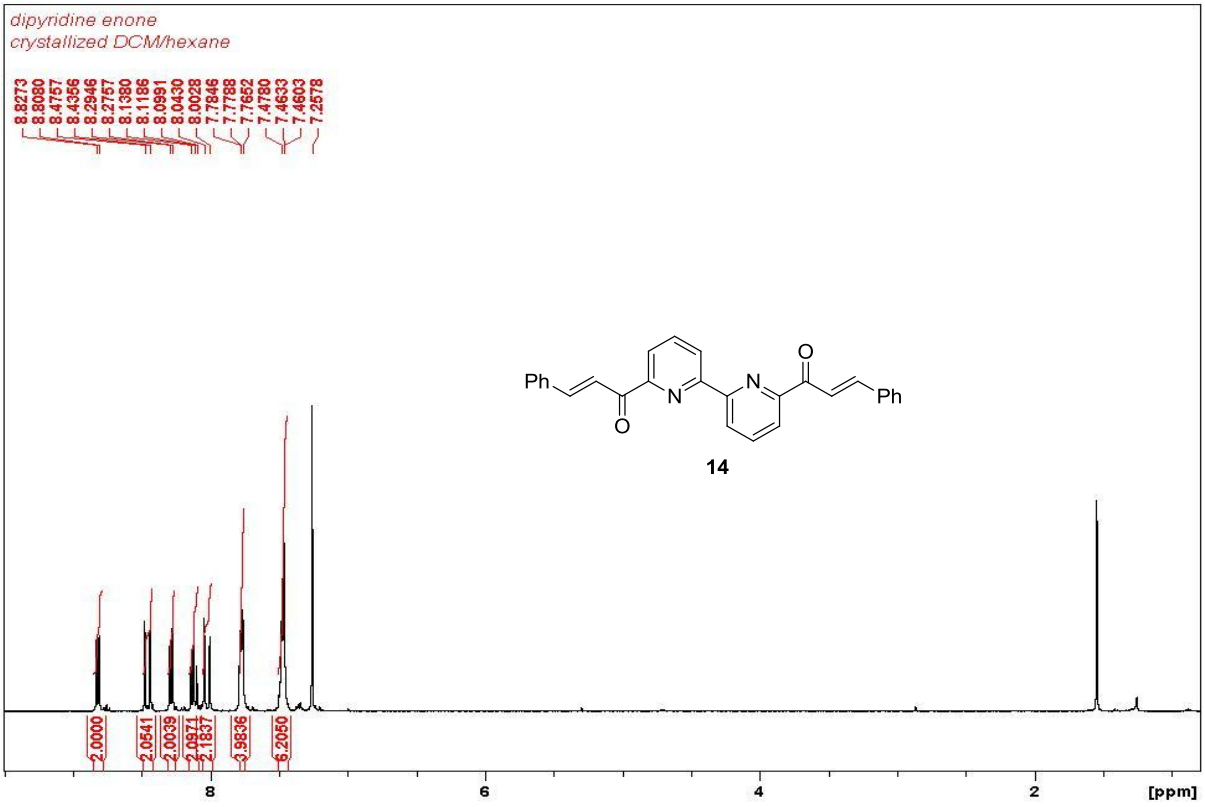

Figure s18. [1]H NMR spectrum of compound **14**.

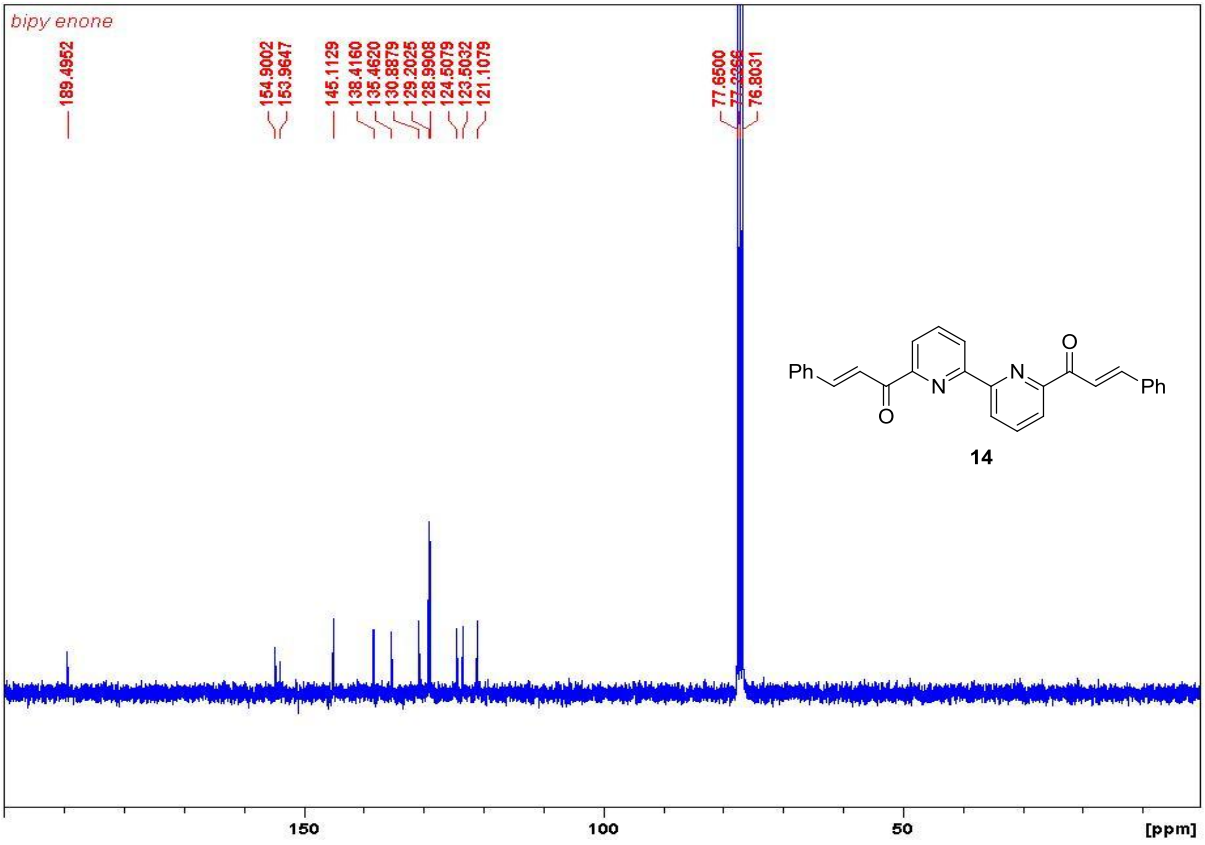

Figure s19. [13]C NMR spectrum of compound **14**.

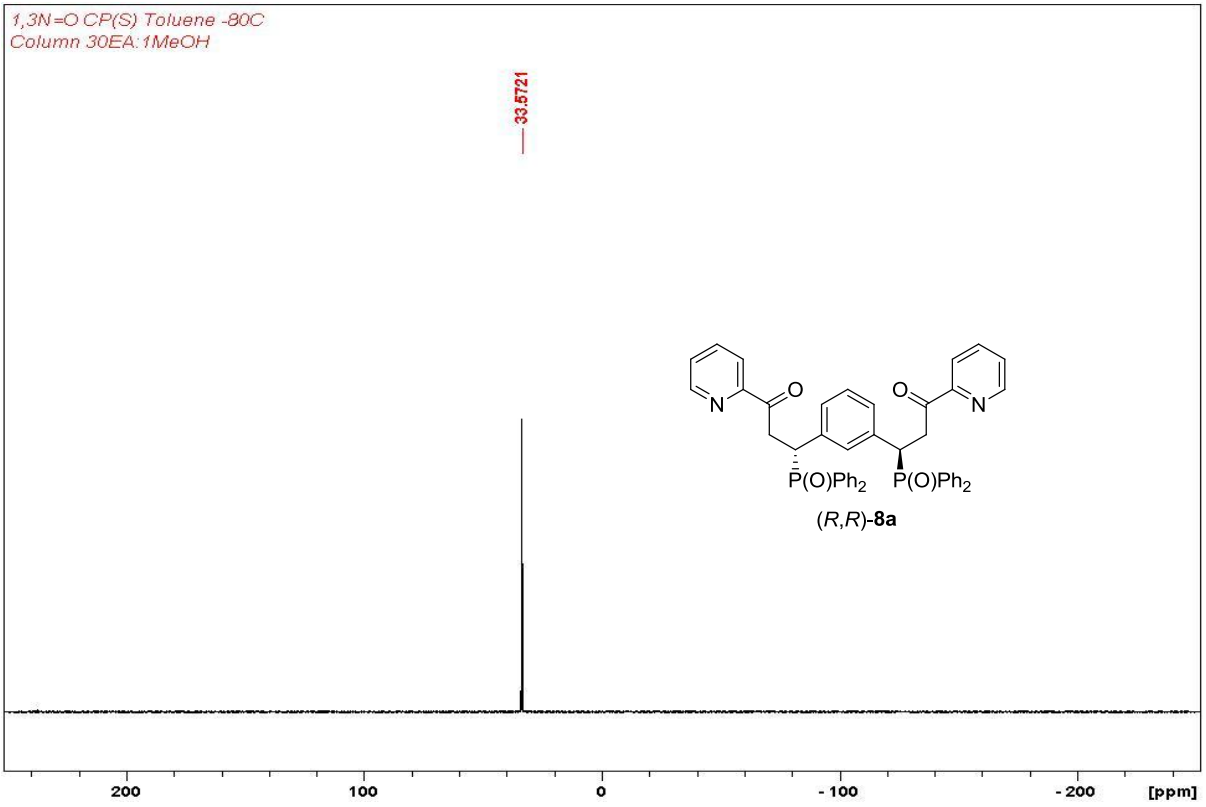

Figure s20. $^{31}P\{^{1}H\}$ NMR spectrum of compound (*R*,*R*)-**8a**.

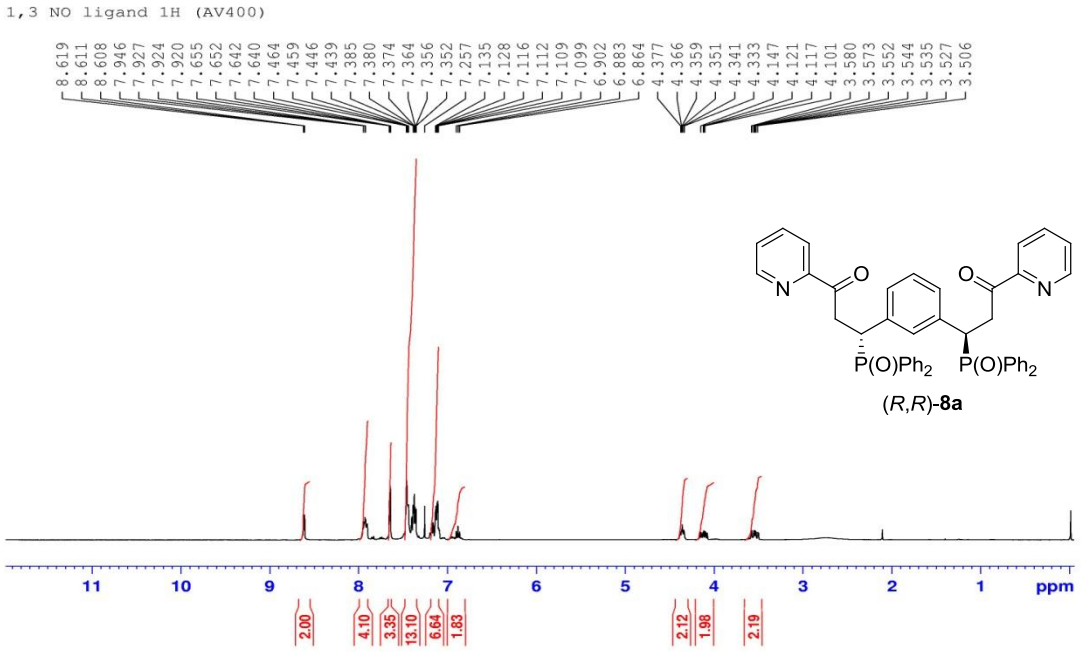

Figure s21. ^{1}H NMR spectrum of compound (*R*,*R*)-**8a**.

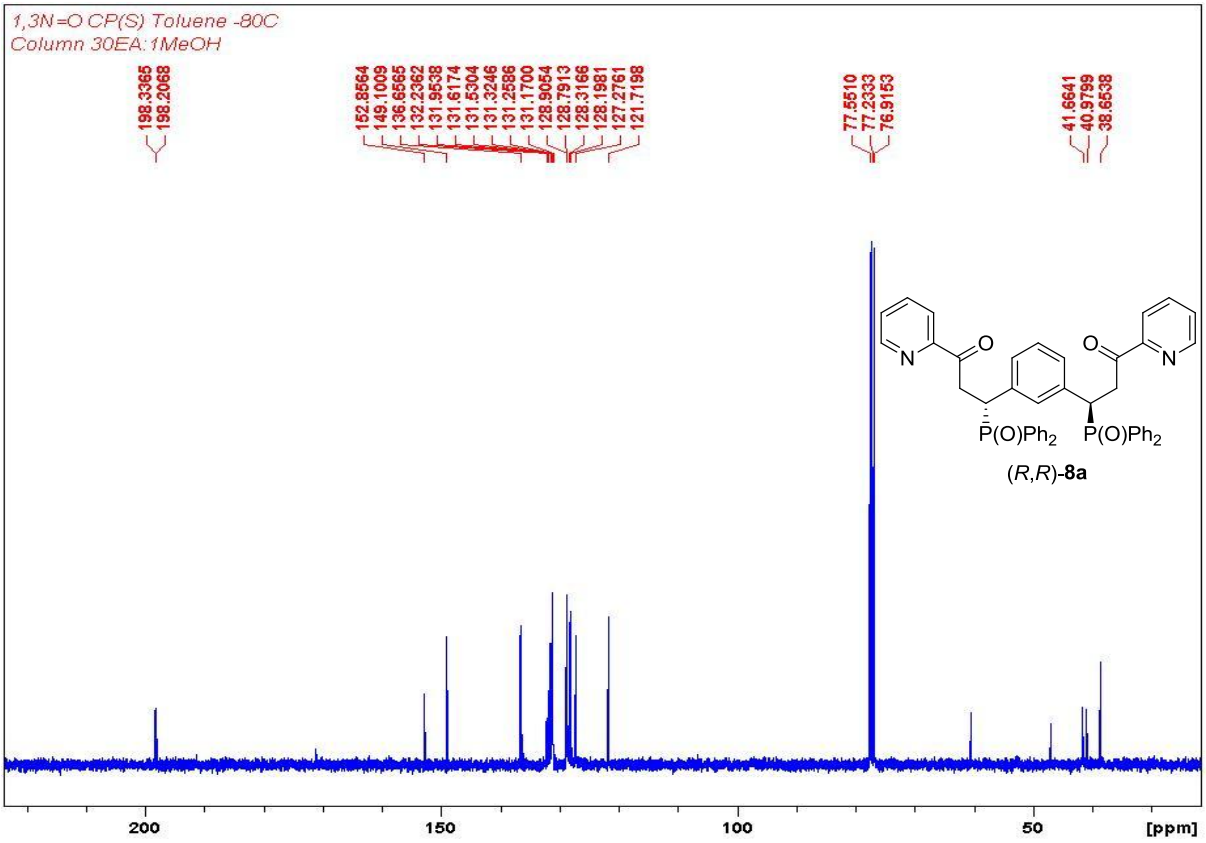

Figure s22. ^{13}C NMR spectrum of compound (*R*,*R*)-**8a**.

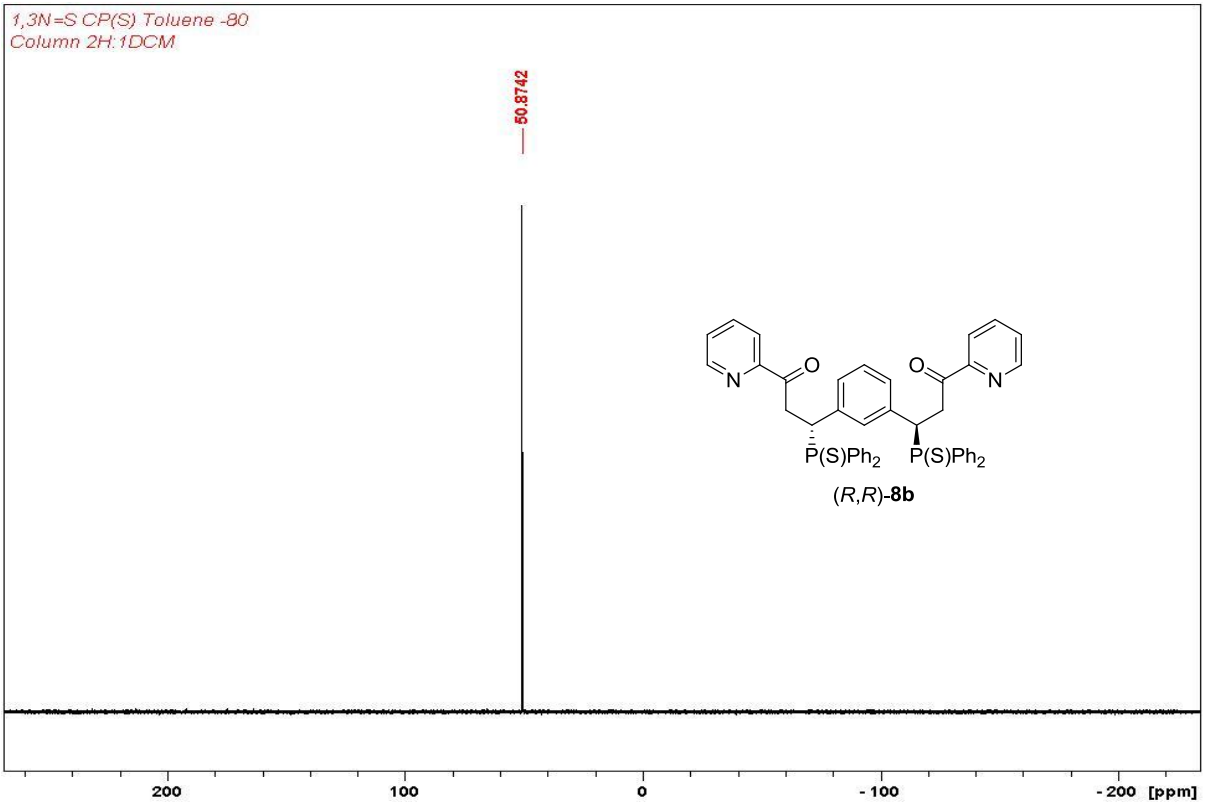

Figure s23. $^{31}P\{^{1}H\}$ NMR spectrum of compound (*R*,*R*)-**8b**.

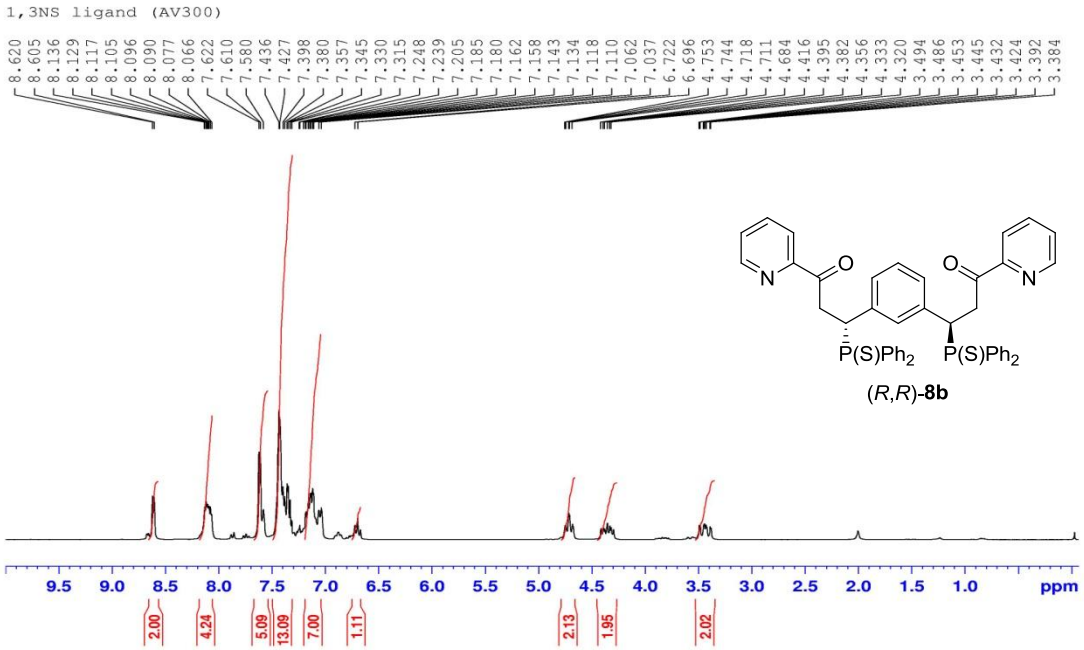

Figure s24. [1]H NMR spectrum of compound (*R*,*R*)-**8b**.

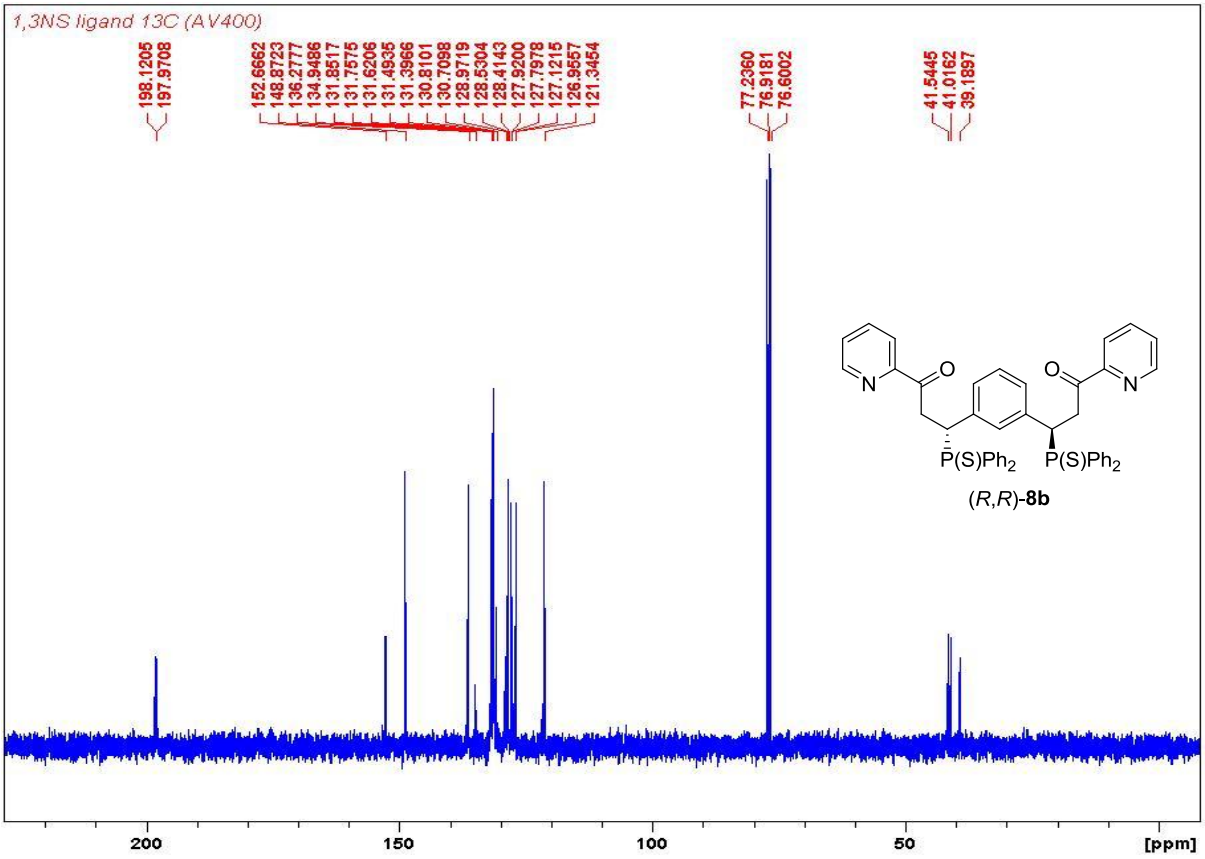

Figure s25. [13]C NMR spectrum of compound (*R*,*R*)-**8b**.

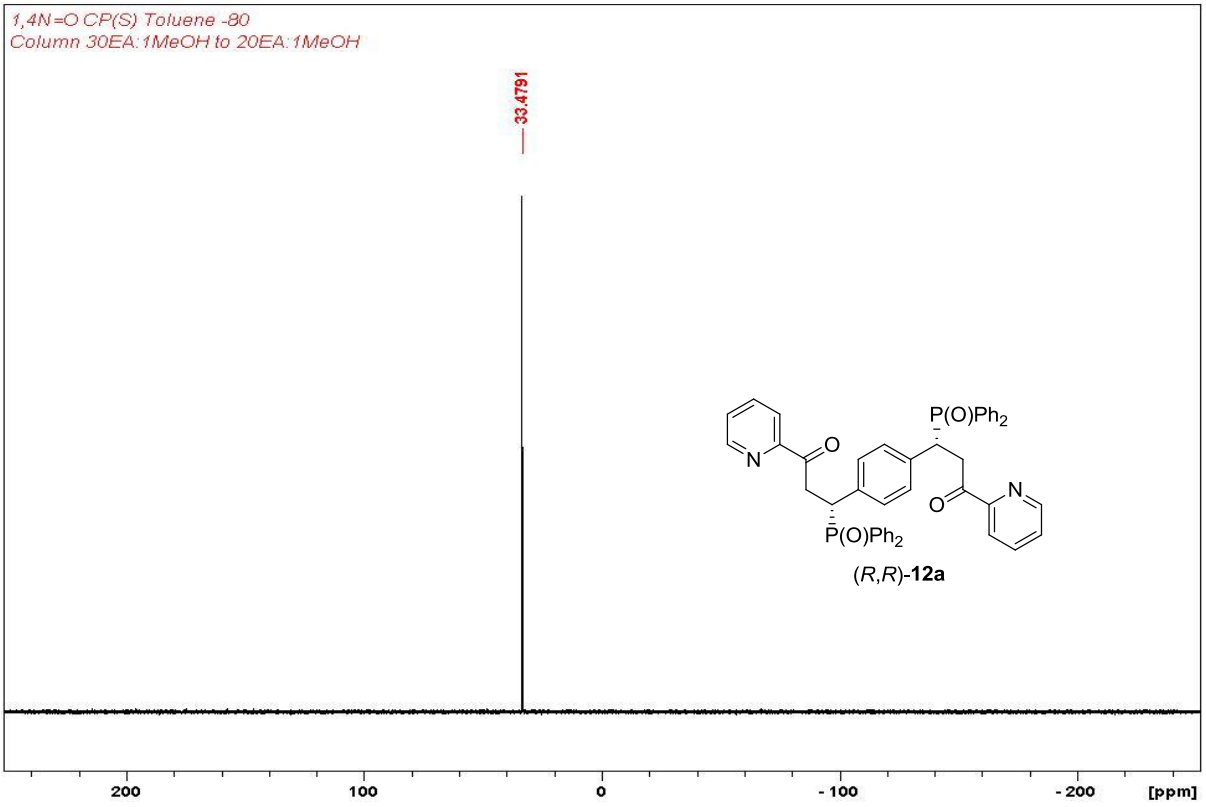

Figure s26. $^{31}P\{^{1}H\}$ NMR spectrum of compound (*R*,*R*)-**12a**.

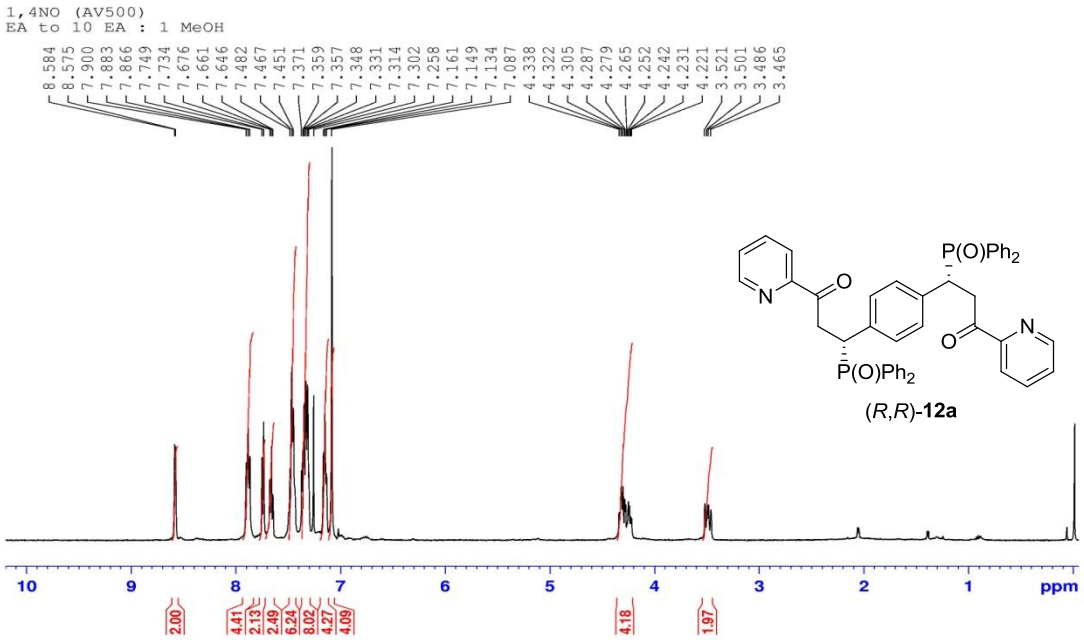

Figure s27. ^{1}H NMR spectrum of compound (*R*,*R*)-**12a**.

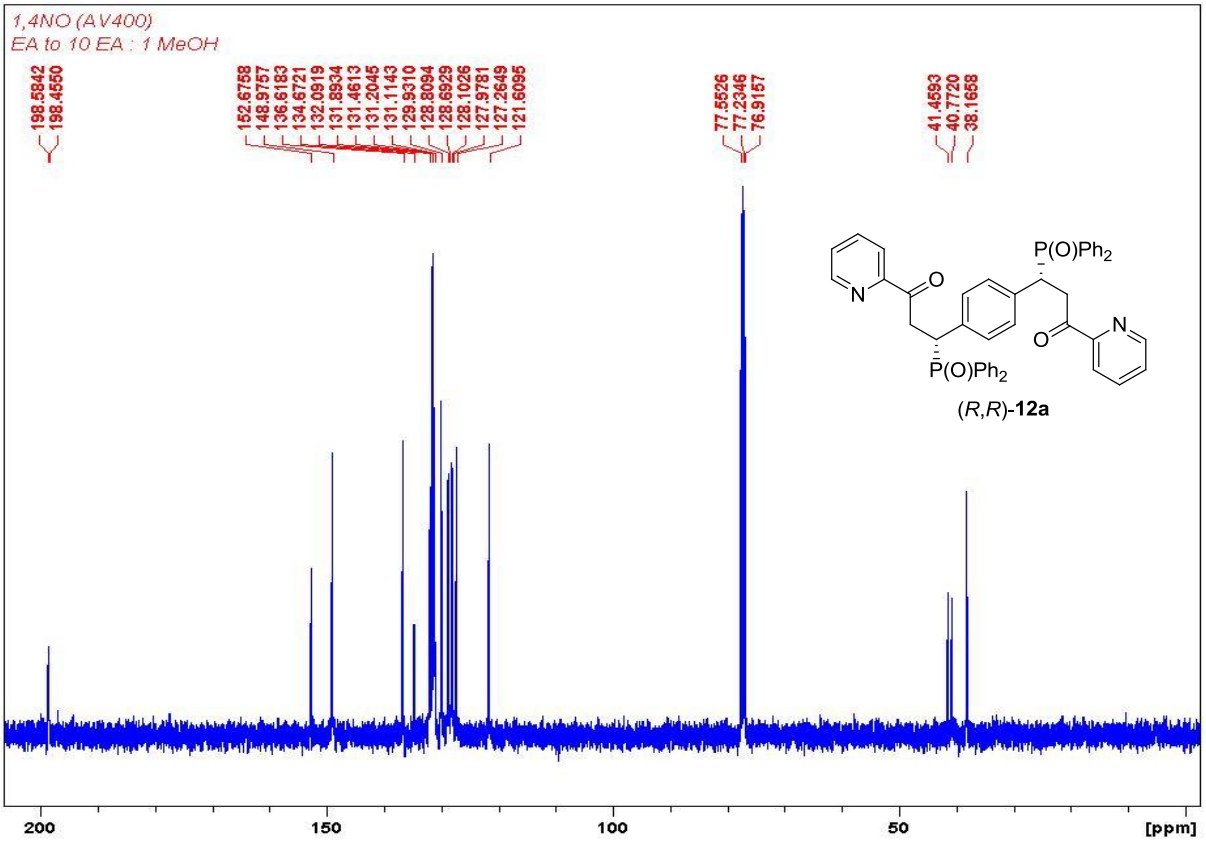

Figure s28. ^{13}C NMR spectrum of compound (*R*,*R*)-**12a**.

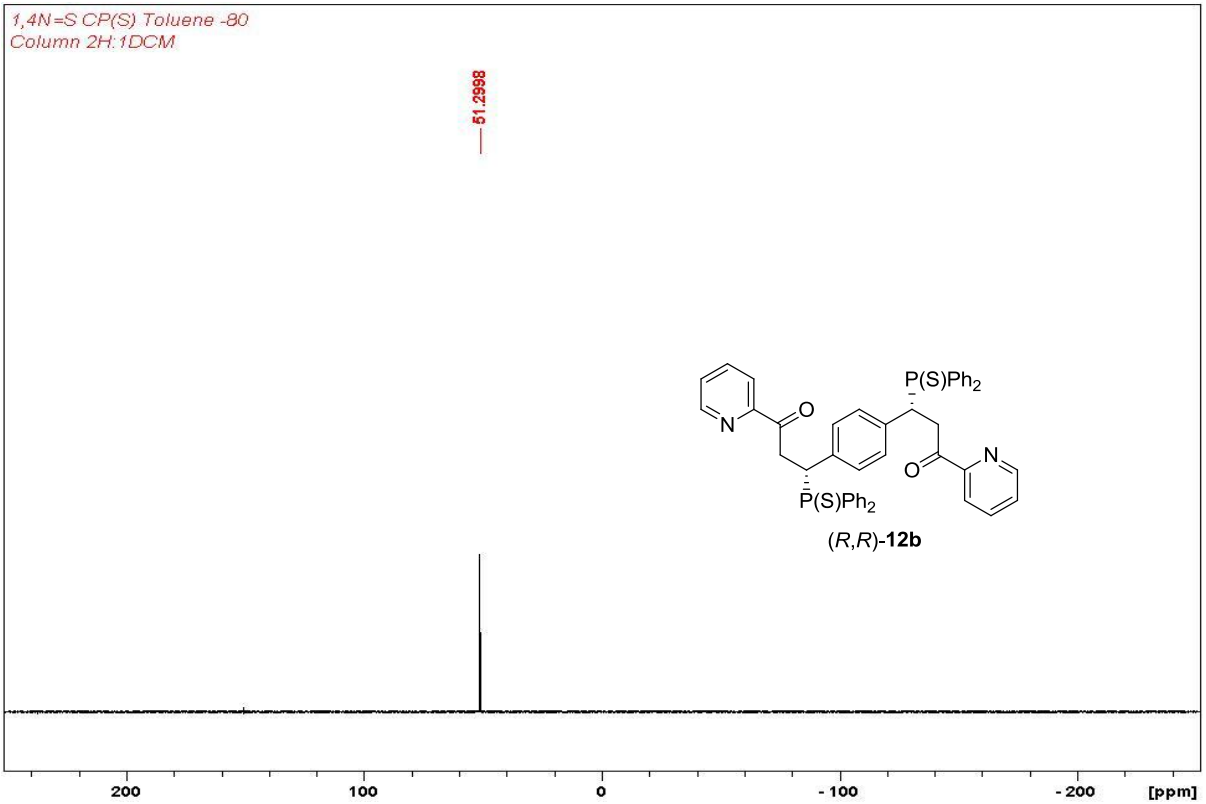

Figure s29. $^{31}P\{^{1}H\}$ NMR spectrum of compound (*R*,*R*)-**12b**.

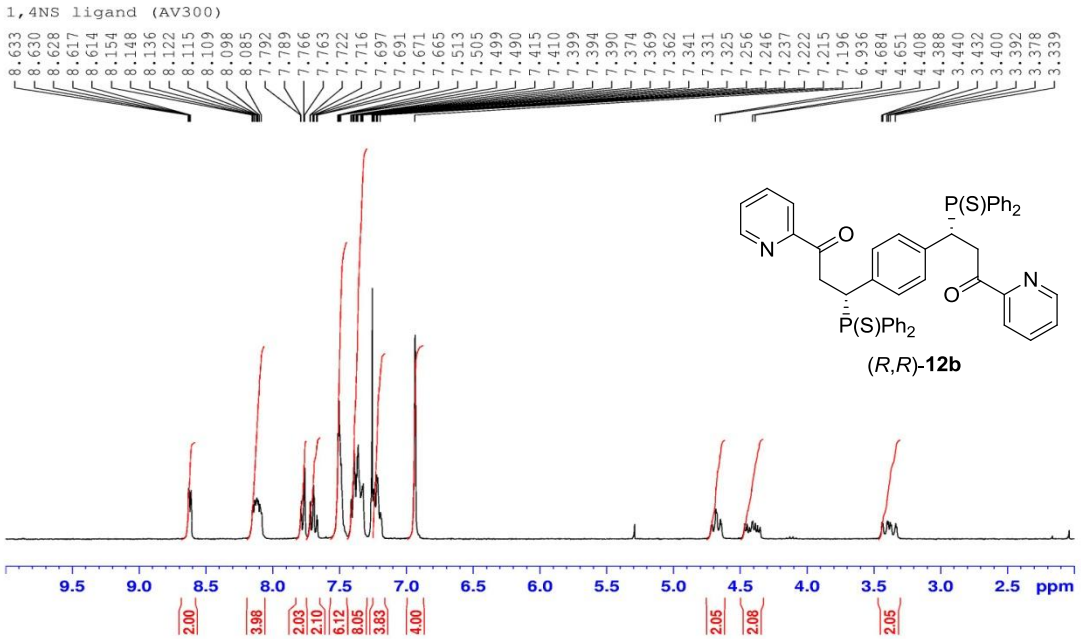

Figure s30. [1]H NMR spectrum of compound (*R*,*R*)-**12b**.

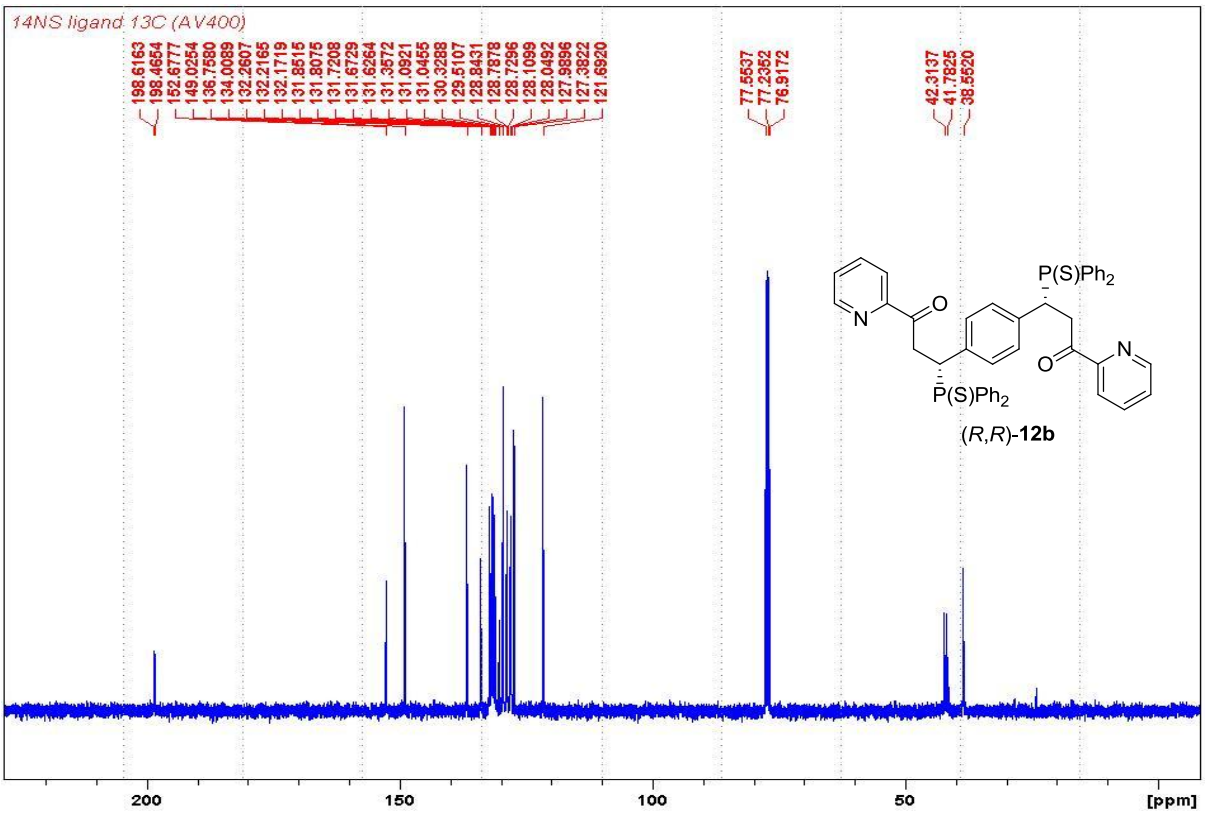

Figure s31. [13]C NMR spectrum of compound (*R*,*R*)-**12b**.

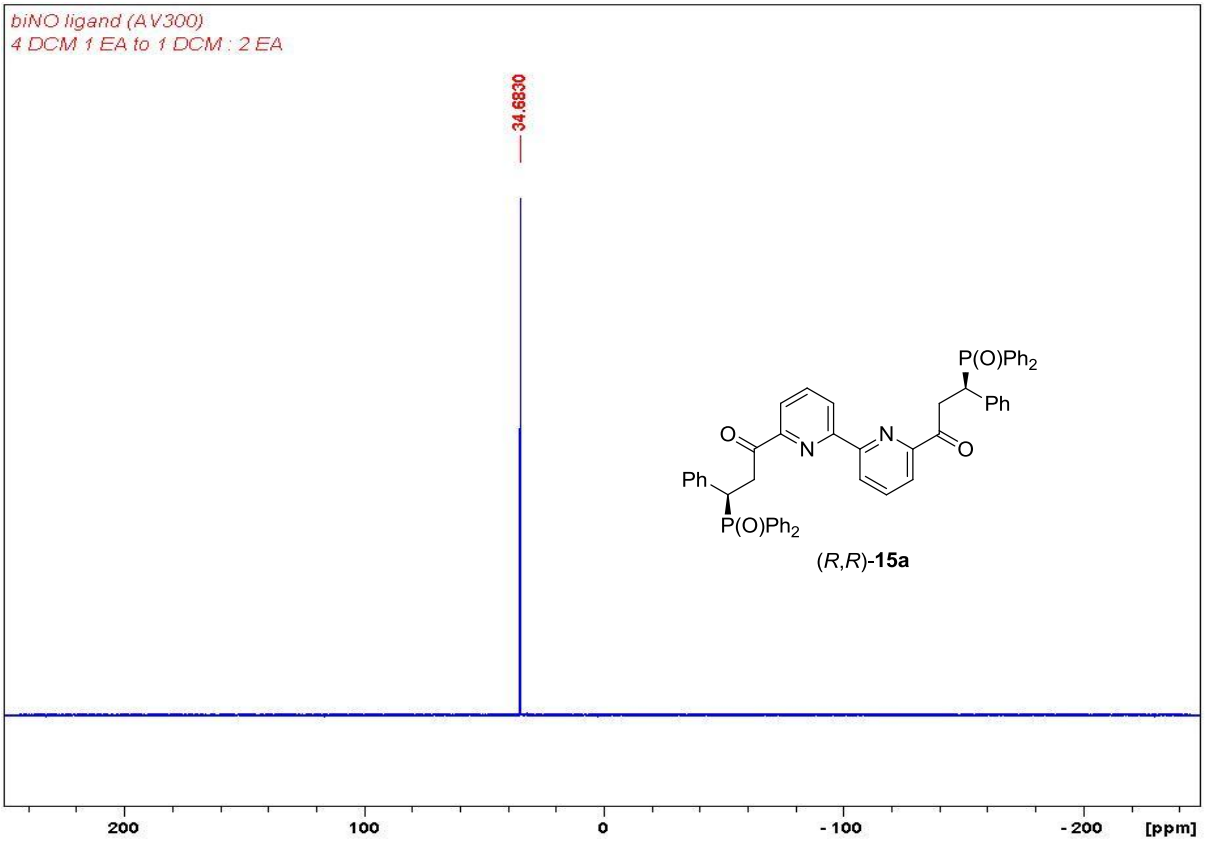

Figure s32. $^{31}P\{^{1}H\}$ NMR spectrum of compound (*R*,*R*)**-15a**.

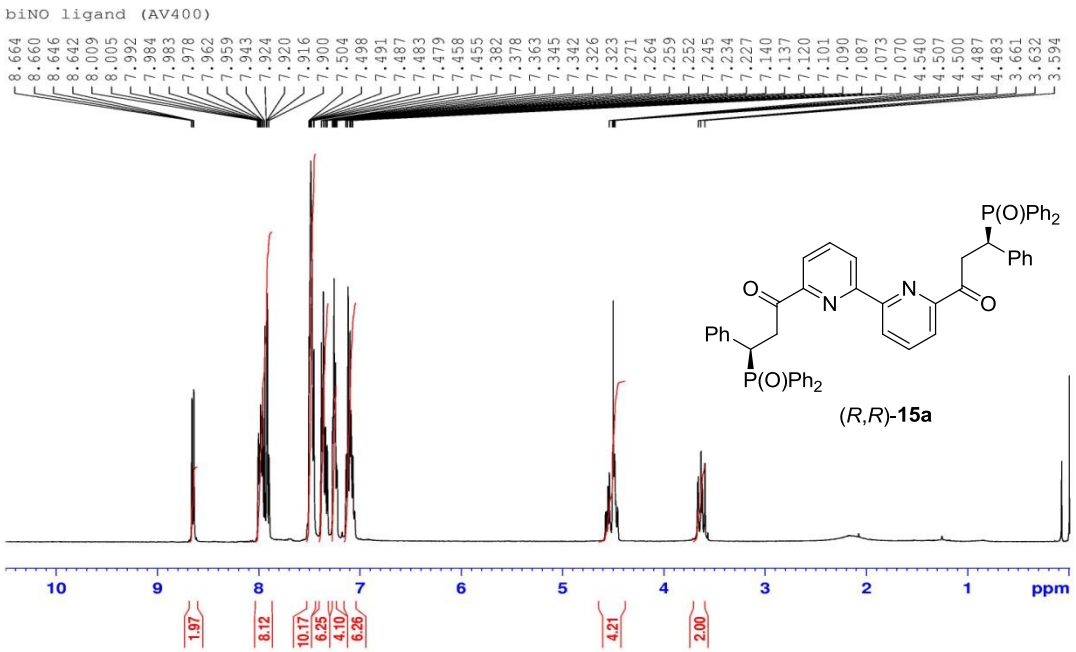

Figure s33. ^{1}H NMR spectrum of compound (*R*,*R*)**-15a**.

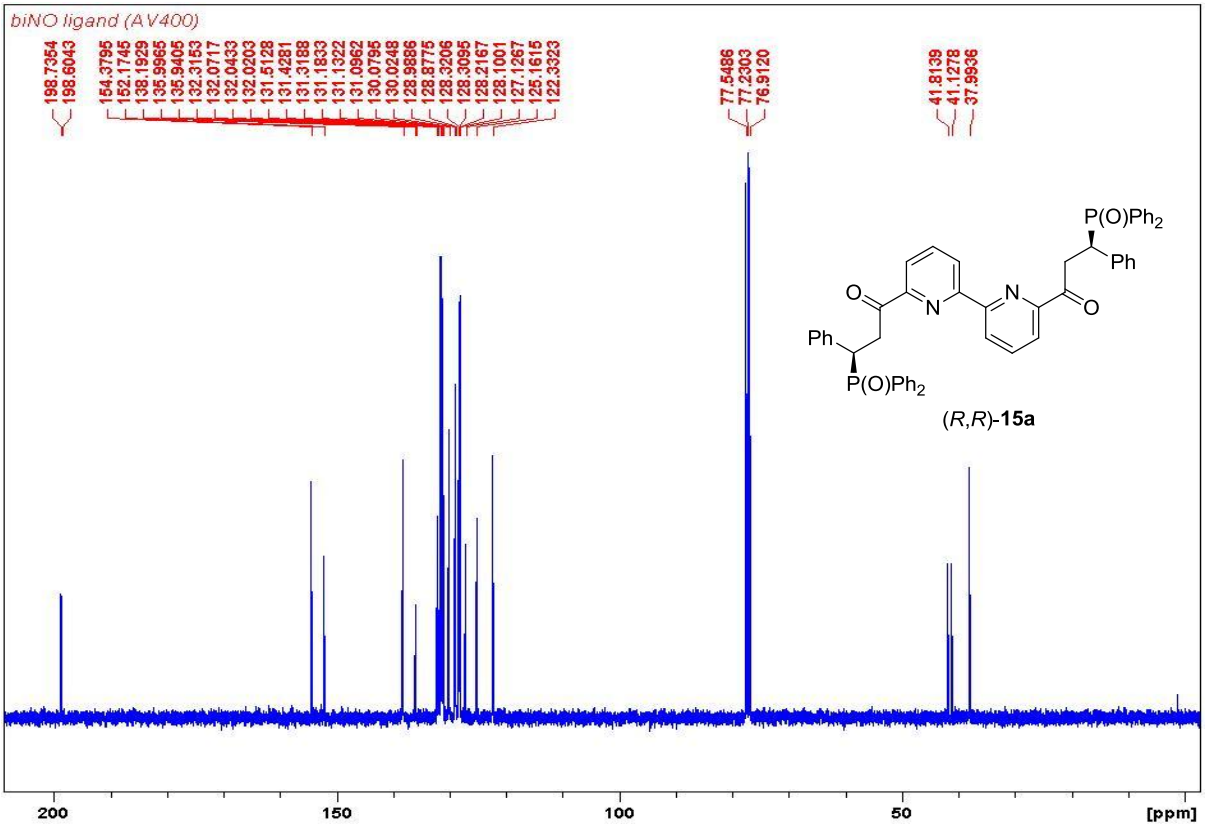

Figure s34. ^{13}C NMR spectrum of compound (*R*,*R*)-**15a**.

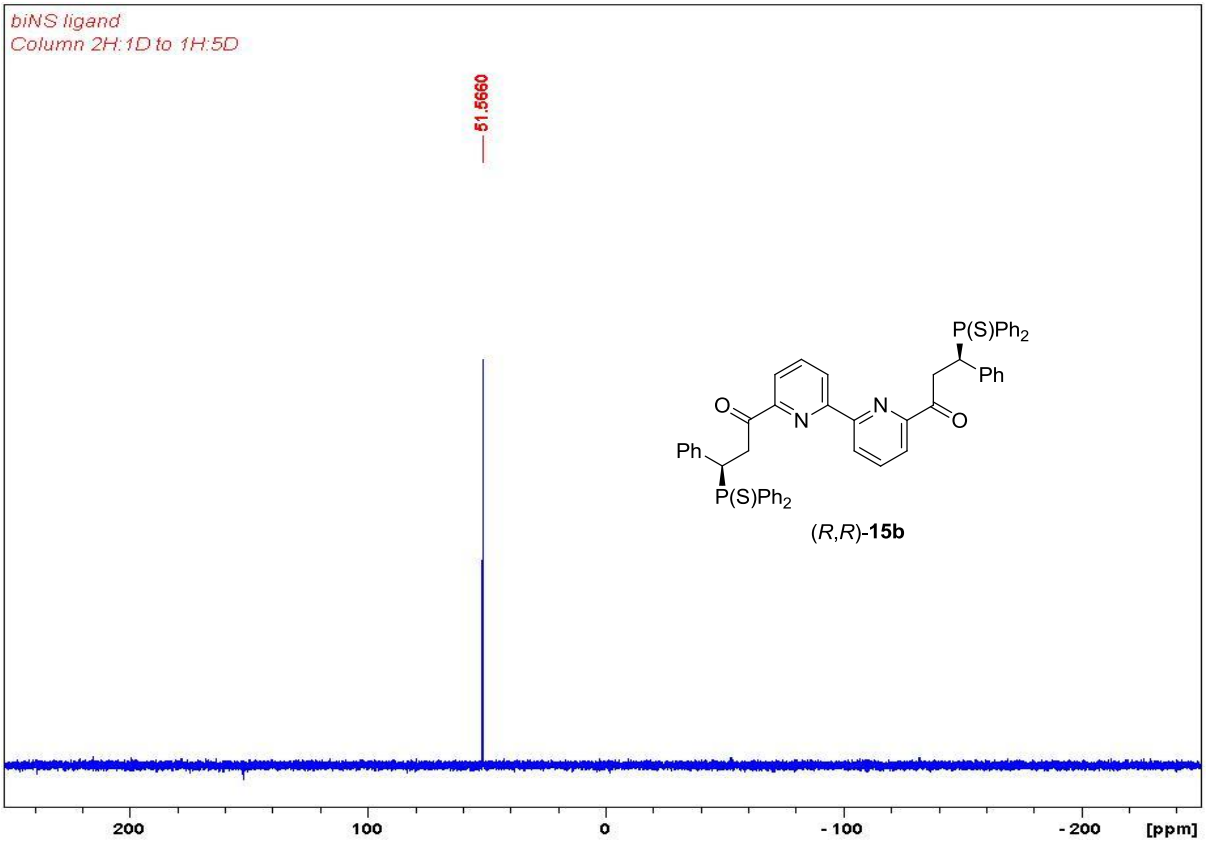

Figure s35. $^{31}P\{^{1}H\}$ NMR spectrum of compound (*R*,*R*)-**15b**.

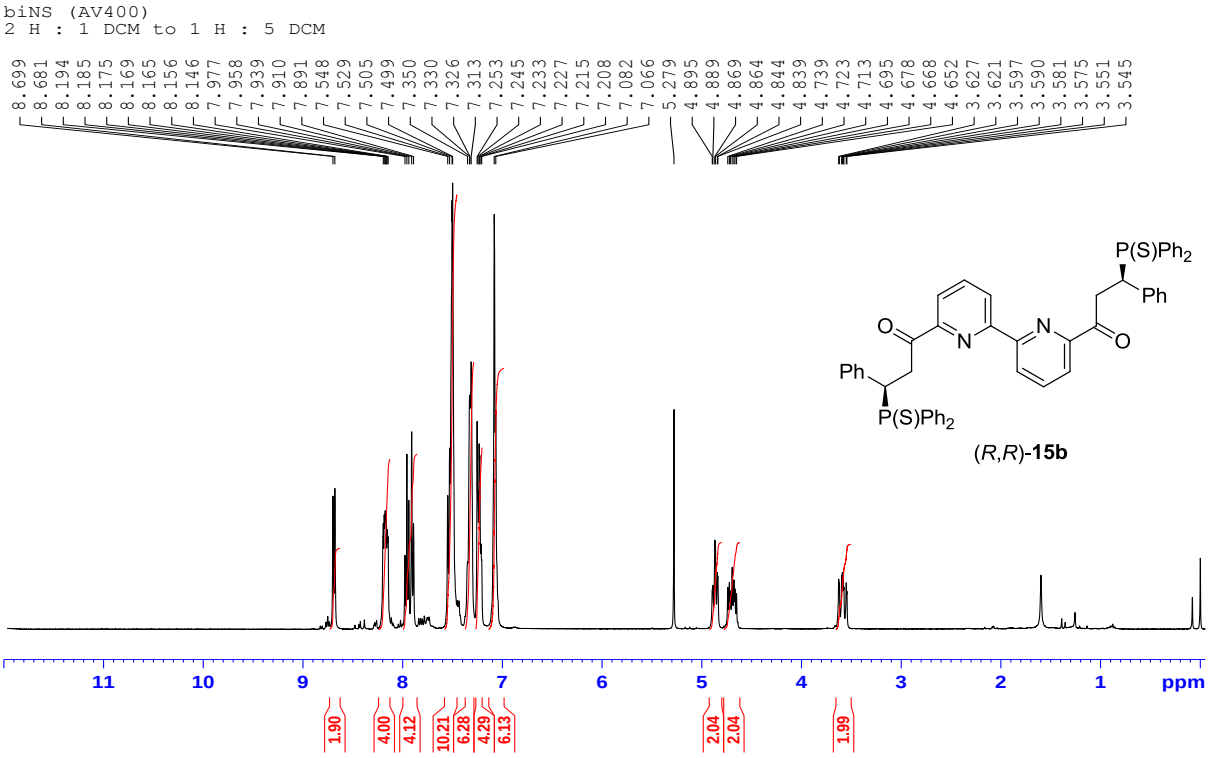

Figure s36. ^{1}H NMR spectrum of compound (*R*,*R*)-**15b**.

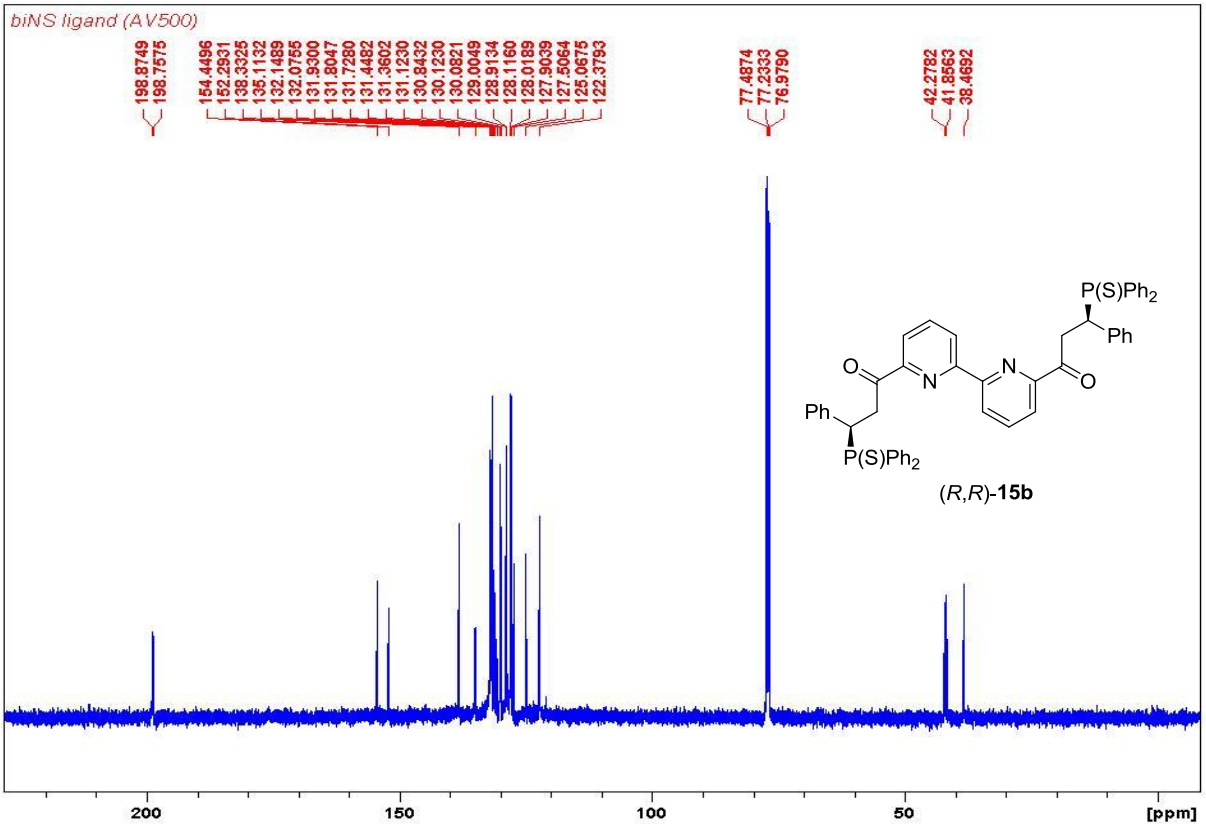

Figure s37. ^{13}C NMR spectrum of compound (*R*,*R*)-**15b**.

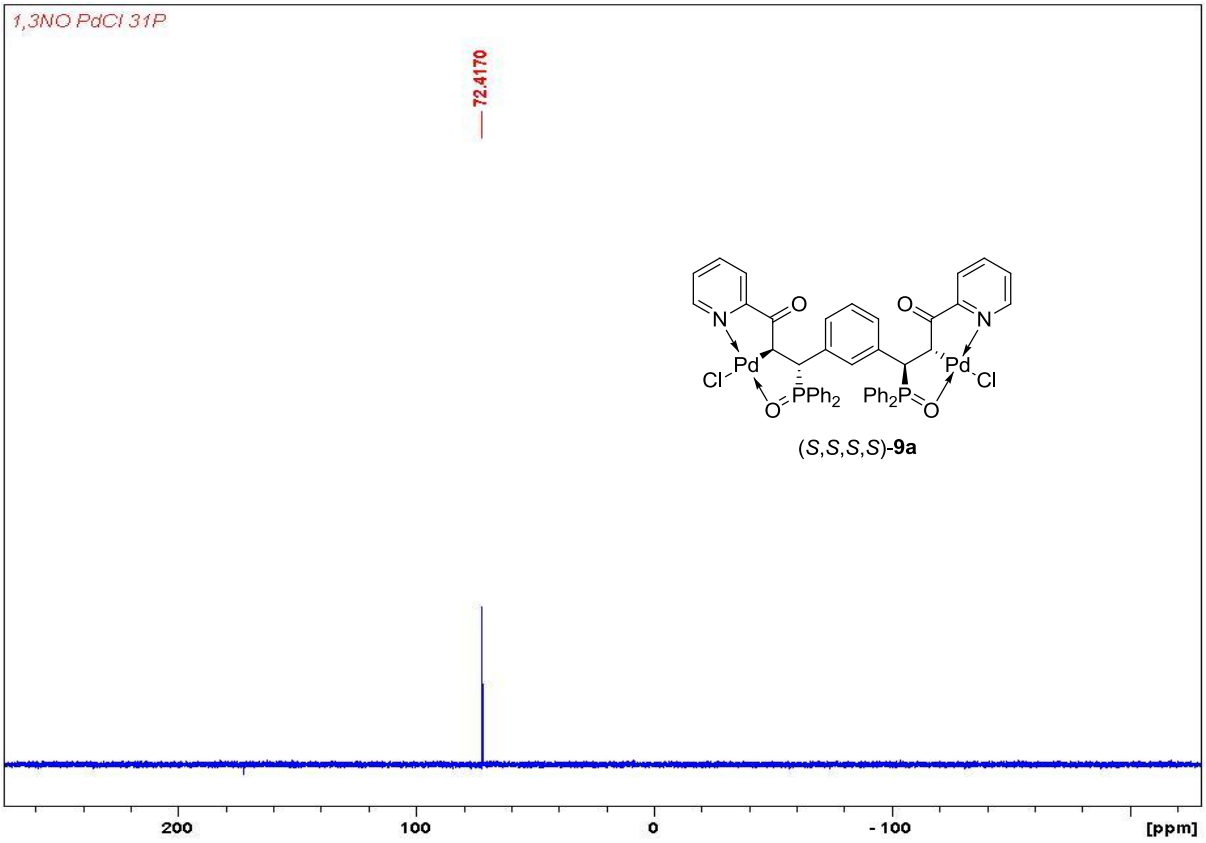

Figure s38. $^{31}P\{^{1}H\}$ NMR spectrum of complex (*S*,*S*,*S*,*S*)-**9a**.

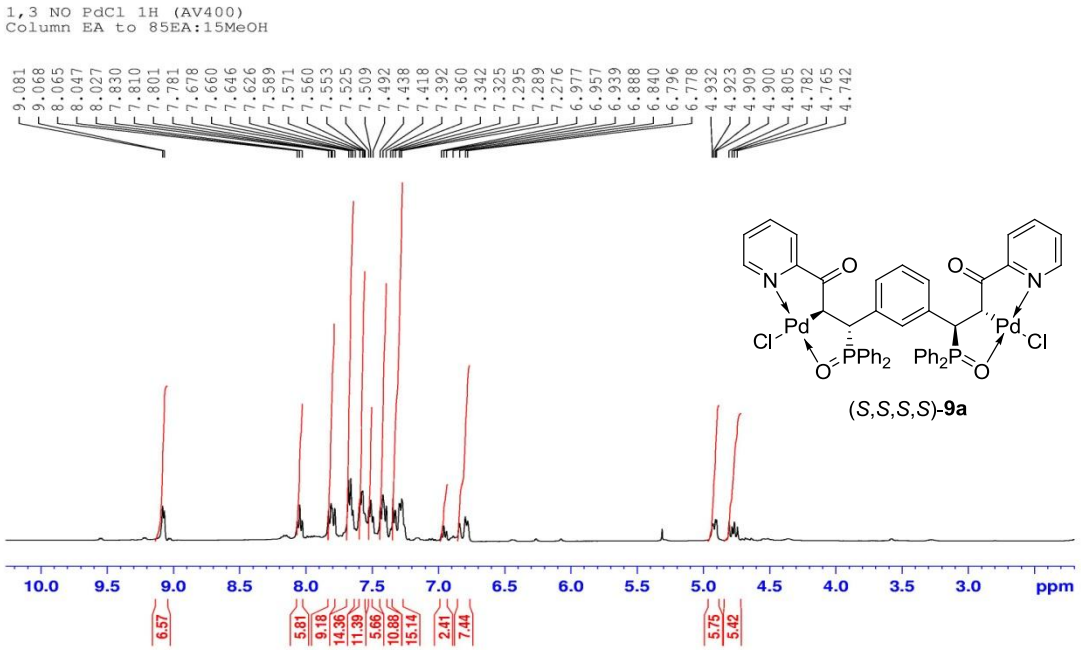

Figure s39. ^{1}H NMR spectrum of complex (*S*,*S*,*S*,*S*)-**9a**.

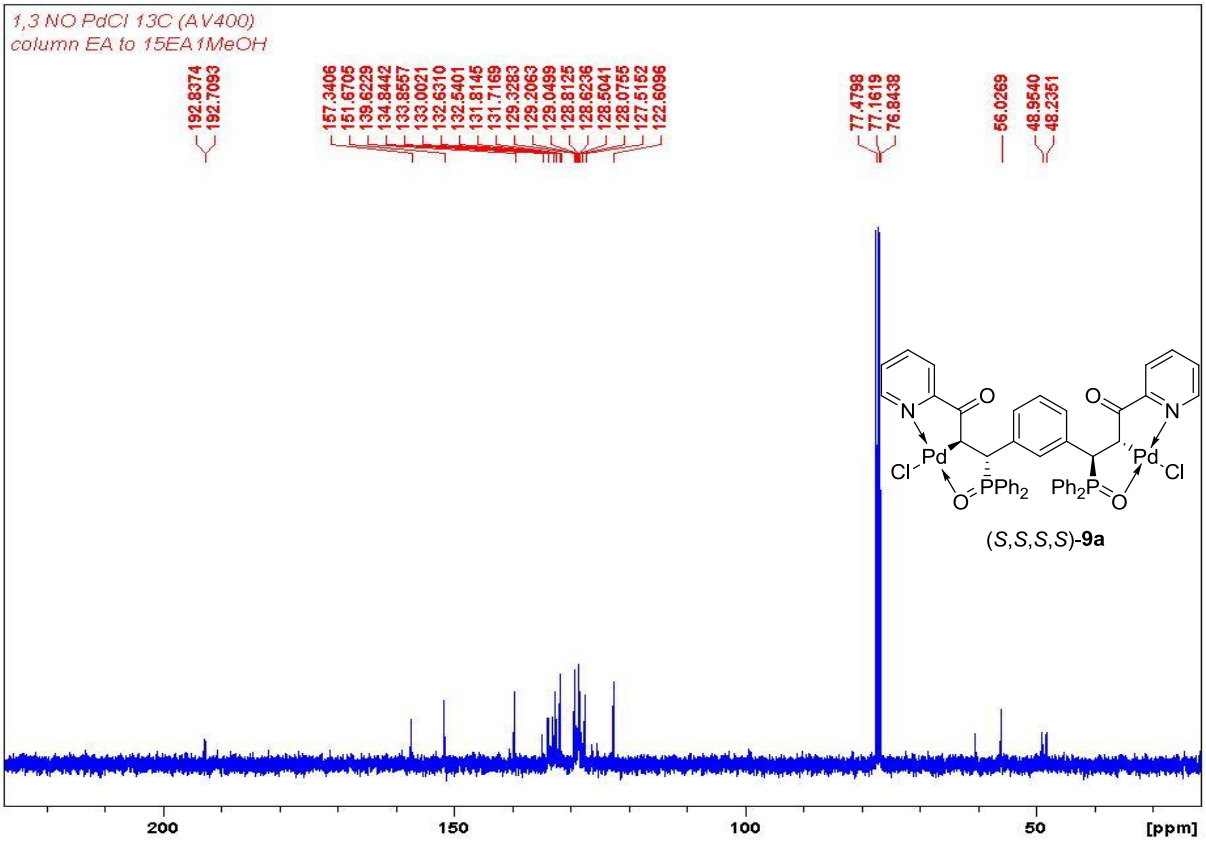

Figure s40. ^{13}C NMR spectrum of complex (*S*,*S*,*S*,*S*)-**9a**.

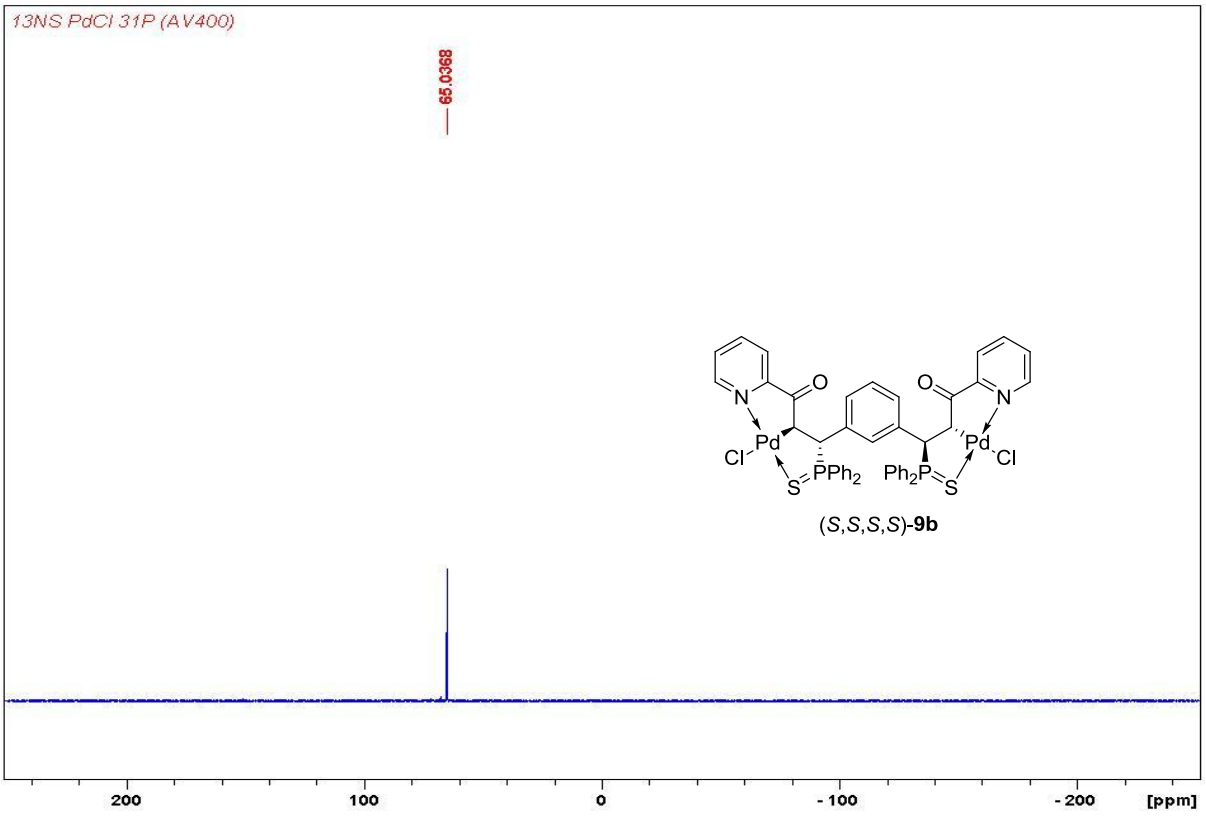

Figure s41. $^{31}P\{^{1}H\}$ NMR spectrum of complex (*S*,*S*,*S*,*S*)-**9b**.

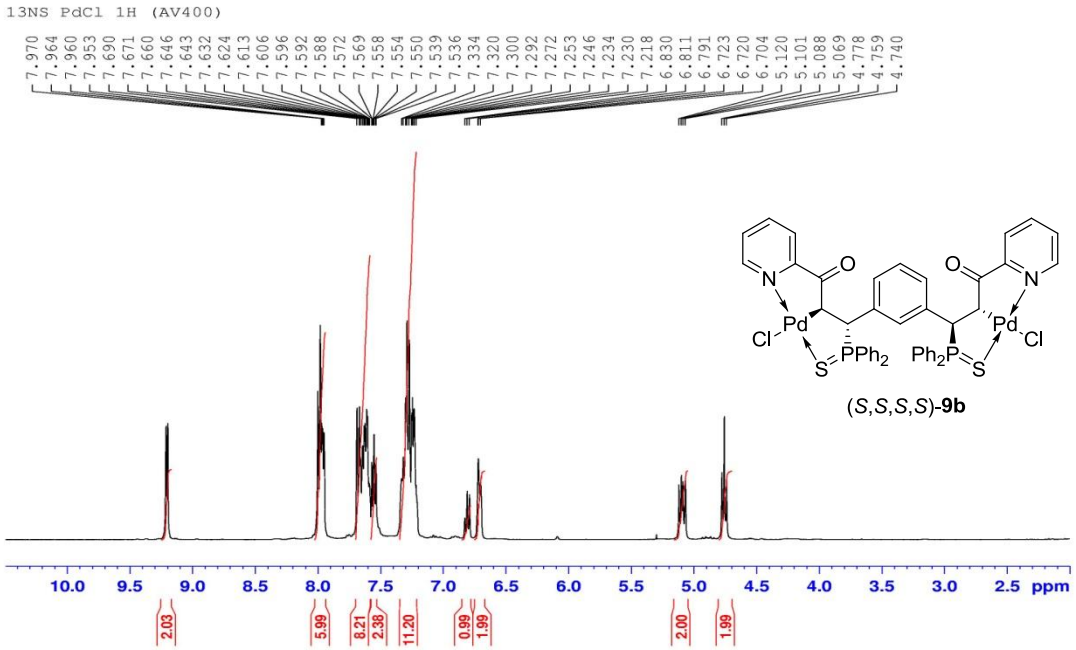

Figure s42. ^{1}H NMR spectrum of complex (*S*,*S*,*S*,*S*)-**9b**.

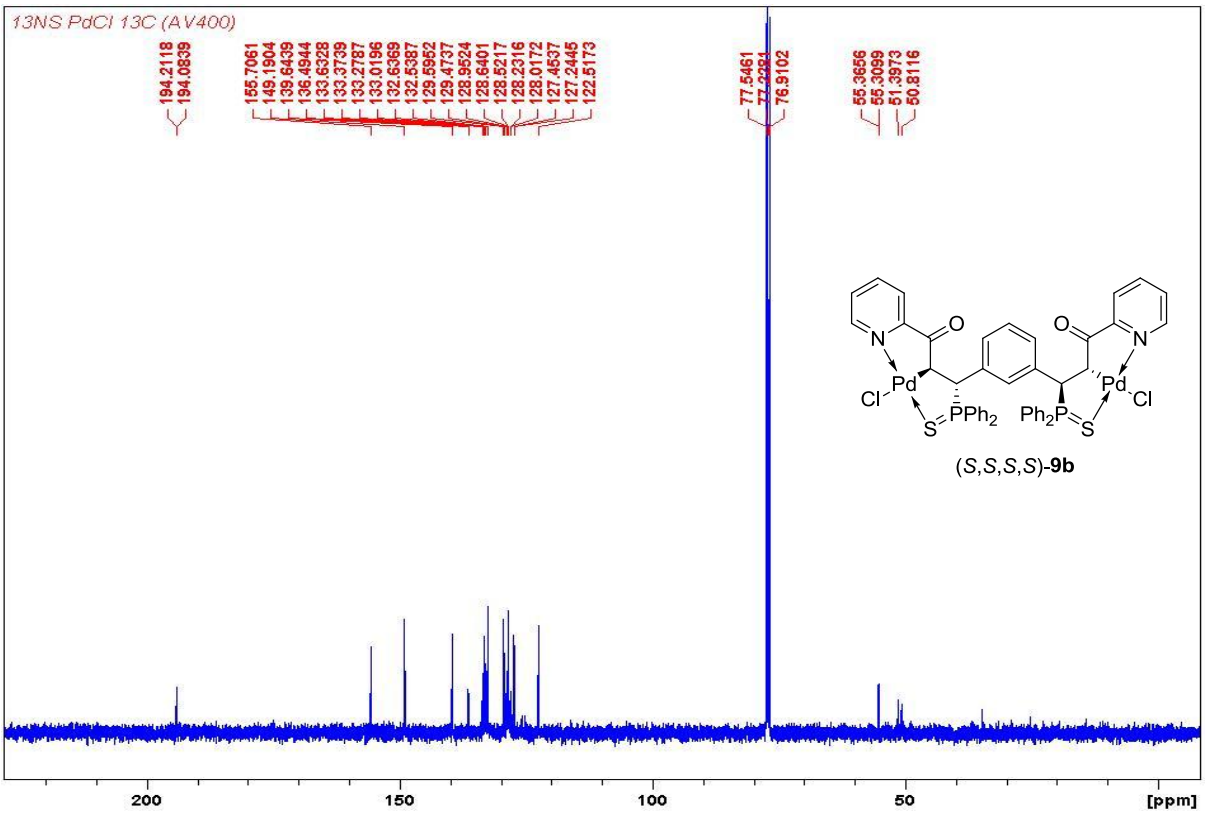

Figure s43. ^{13}C NMR spectrum of complex (*S*,*S*,*S*,*S*)-**9b**.

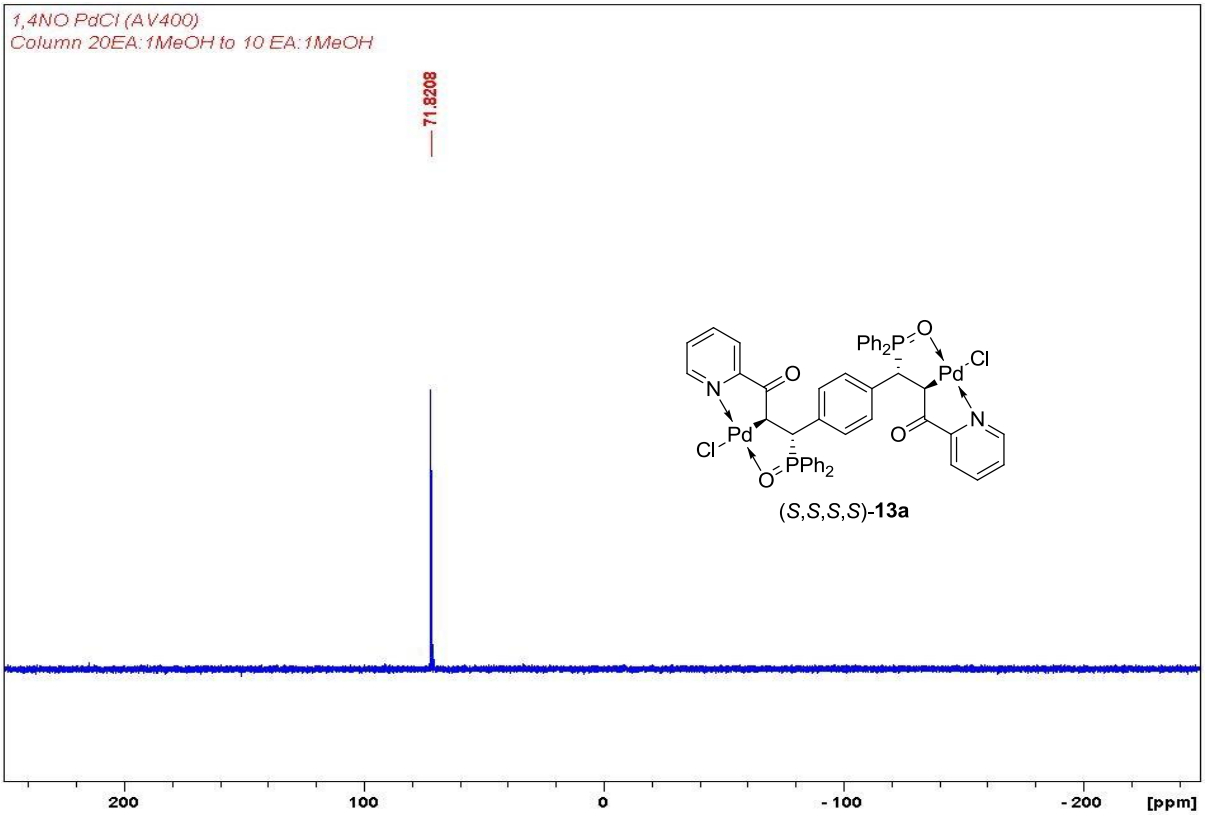

Figure s44. $^{31}P\{^{1}H\}$ NMR spectrum of complex (*S*,*S*,*S*,*S*)-**13a**.

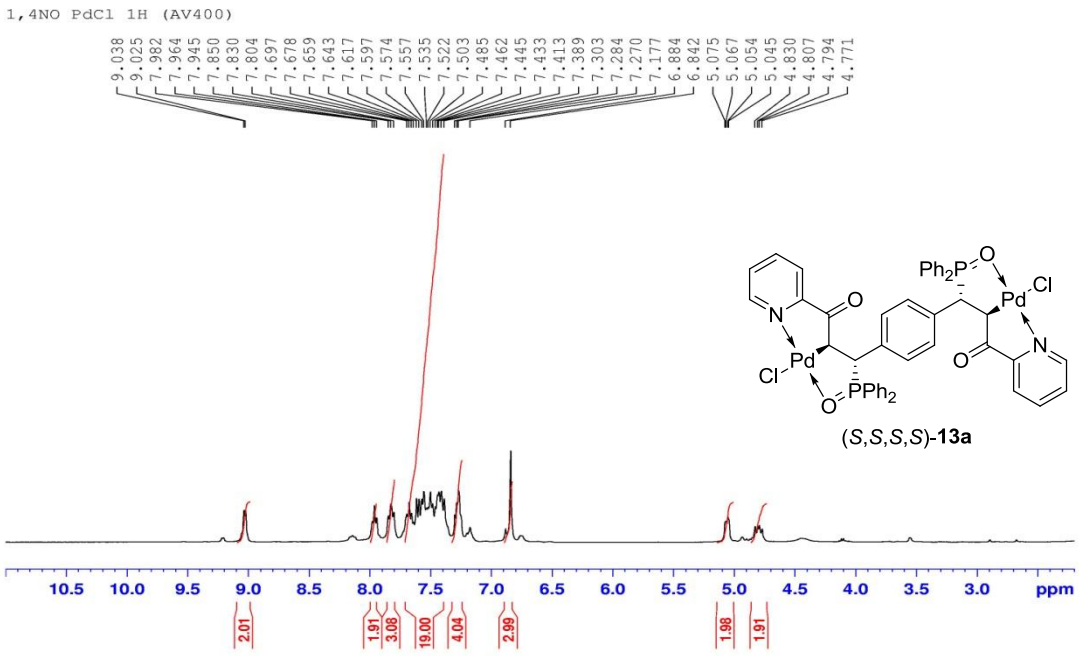

Figure s45. ^{1}H NMR spectrum of complex (*S*,*S*,*S*,*S*)-**13a**.

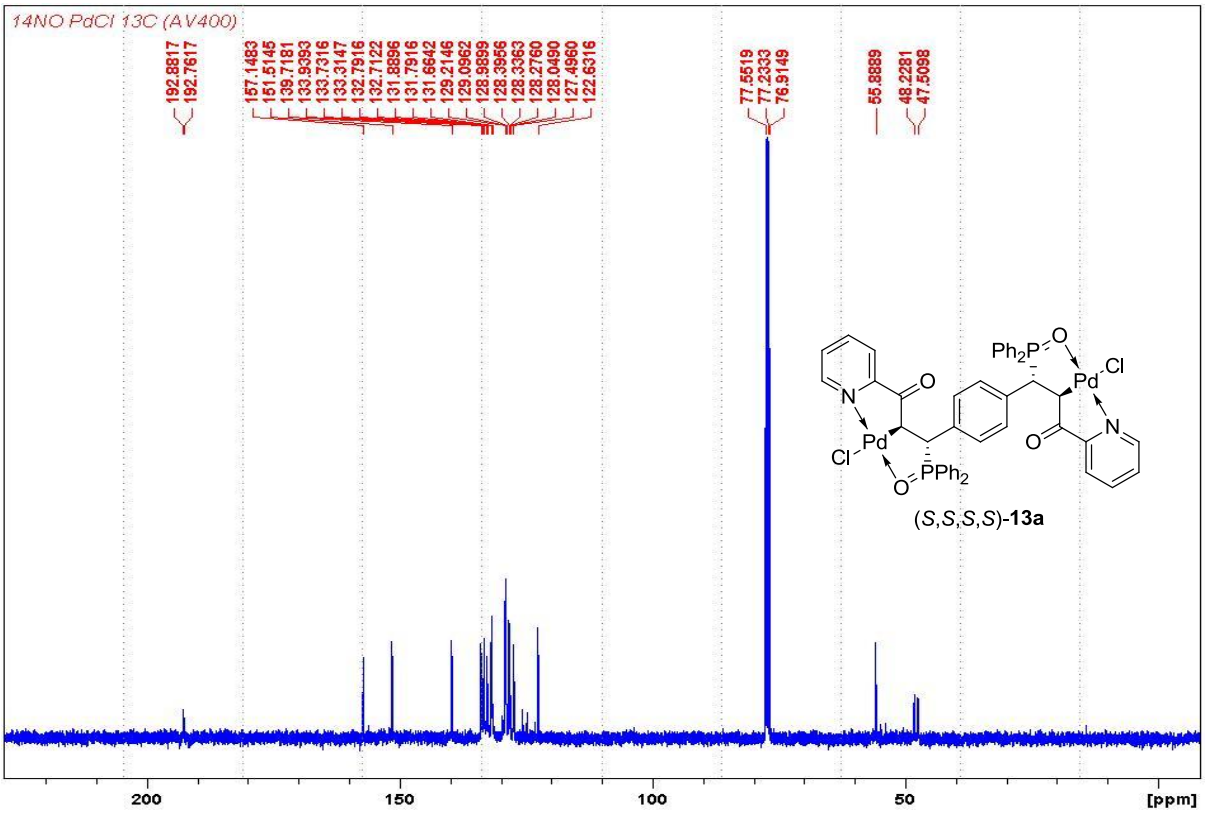

Figure s46. ^{13}C NMR spectrum of complex (*S*,*S*,*S*,*S*)-**13a**.

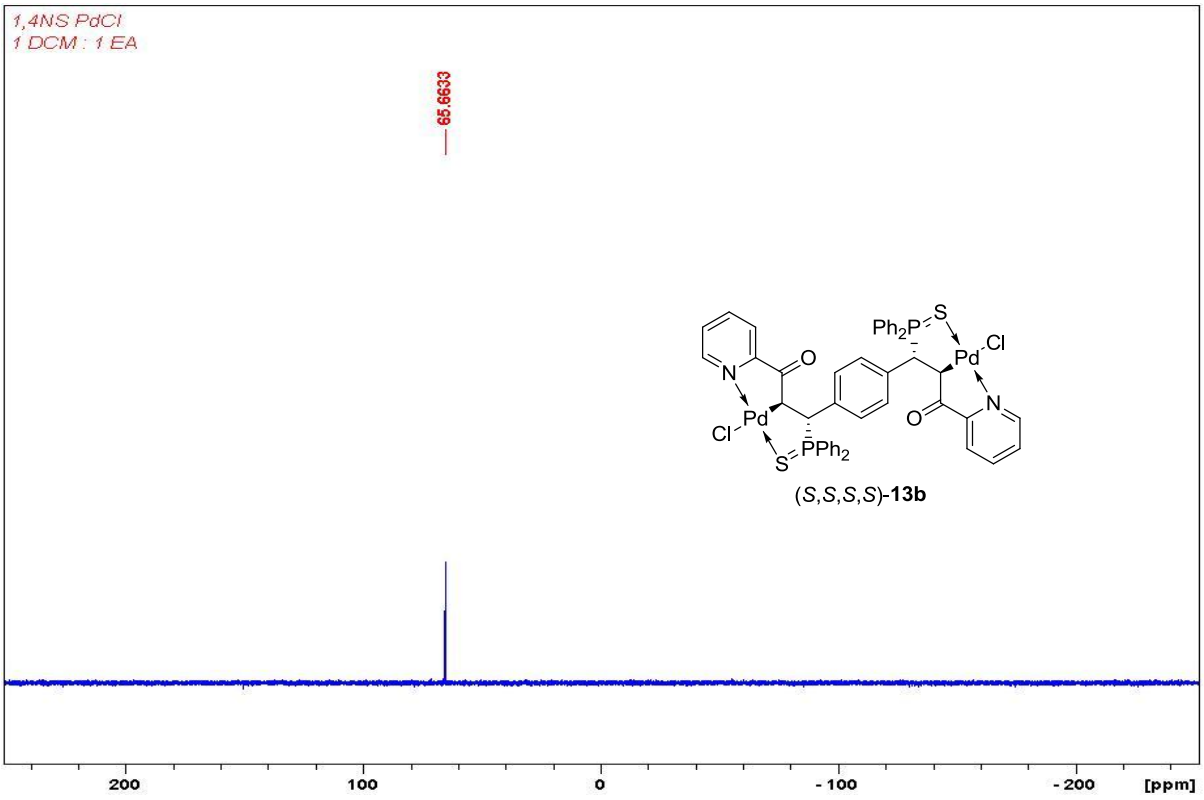

Figure s47. $^{31}P\{^{1}H\}$ NMR spectrum of complex (*S*,*S*,*S*,*S*)-**13b**.

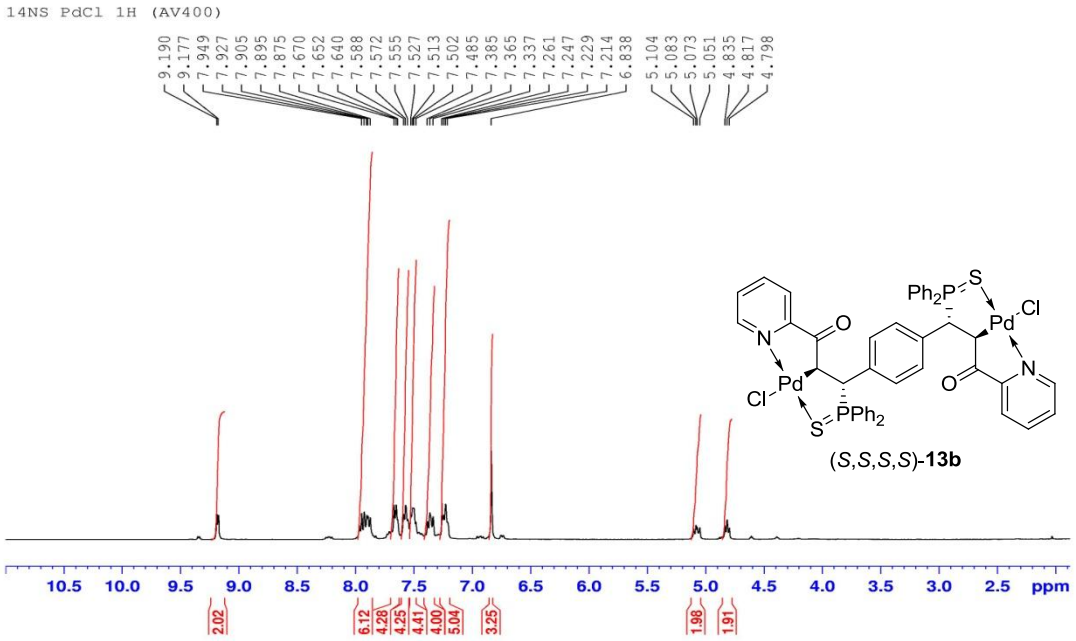

Figure s48. ^{1}H NMR spectrum of complex (*S*,*S*,*S*,*S*)-**13b**.

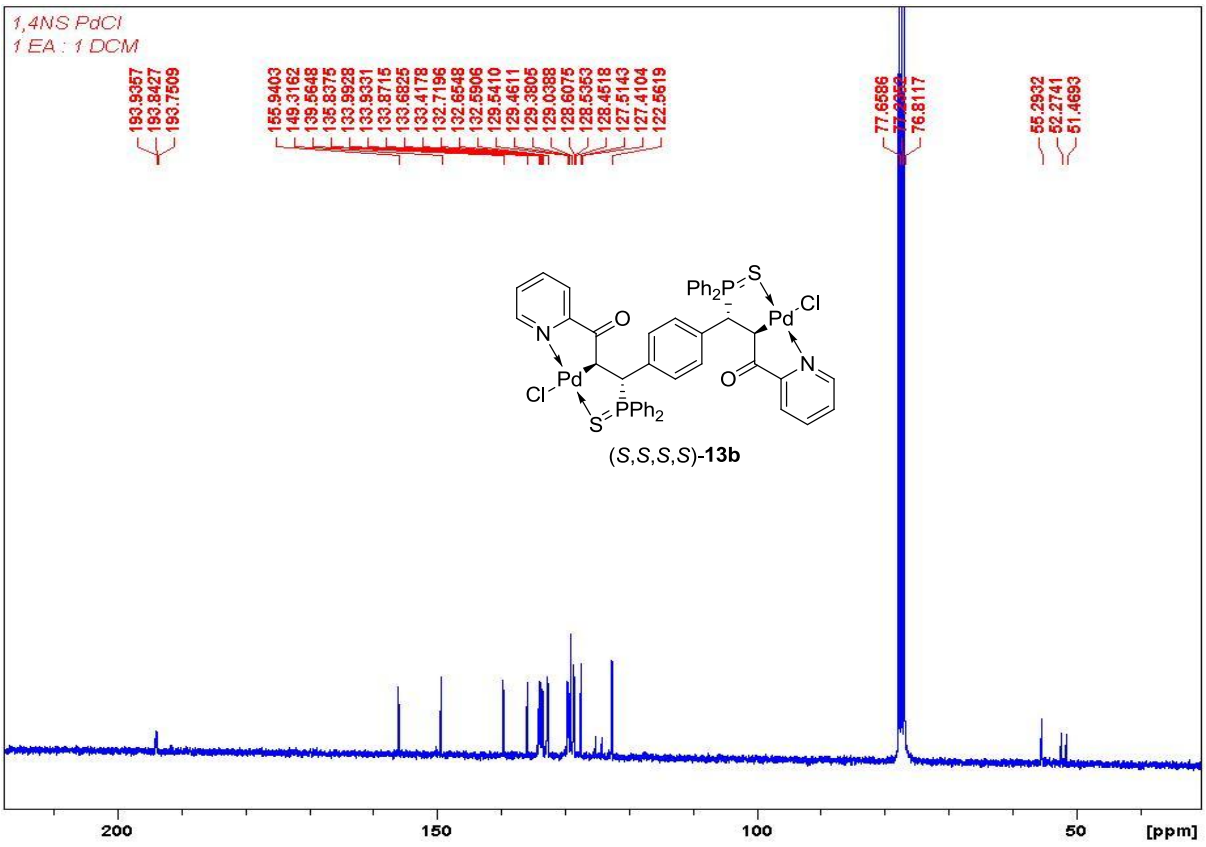

Figure s49. ^{13}C NMR spectrum of complex (*S*,*S*,*S*,*S*)-**13b**.

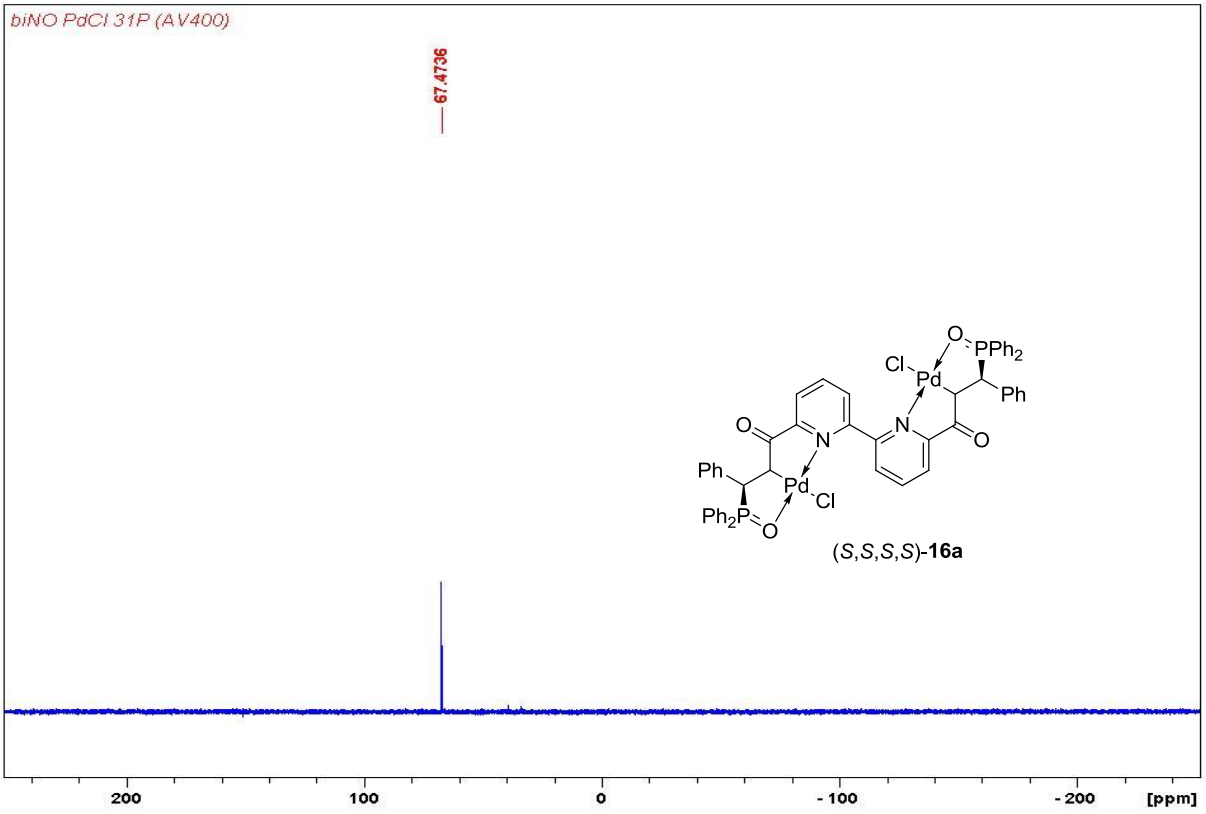

Figure s50. $^{31}P\{^{1}H\}$ NMR spectrum of complex (*S*,*S*,*S*,*S*)-**16a**.

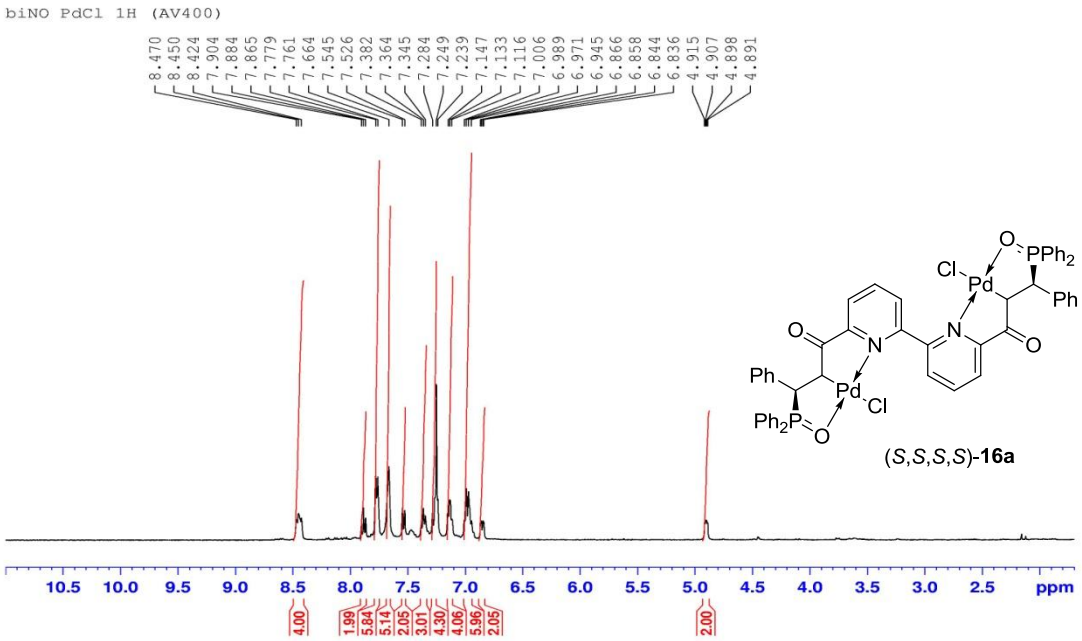

Figure s51. ^{1}H NMR spectrum of complex (*S*,*S*,*S*,*S*)-**16a**.

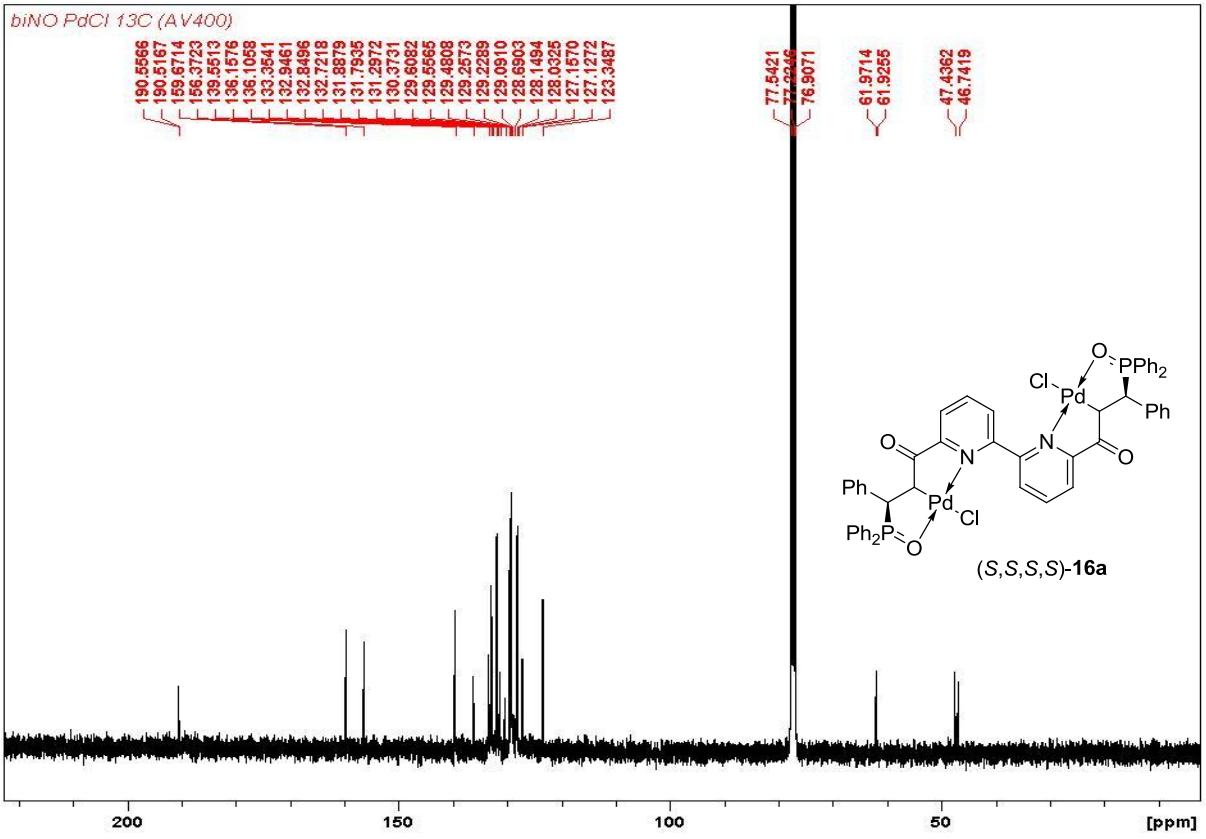

Figure s52. ^{13}C NMR spectrum of complex (*S*,*S*,*S*,*S*)-**16a**.

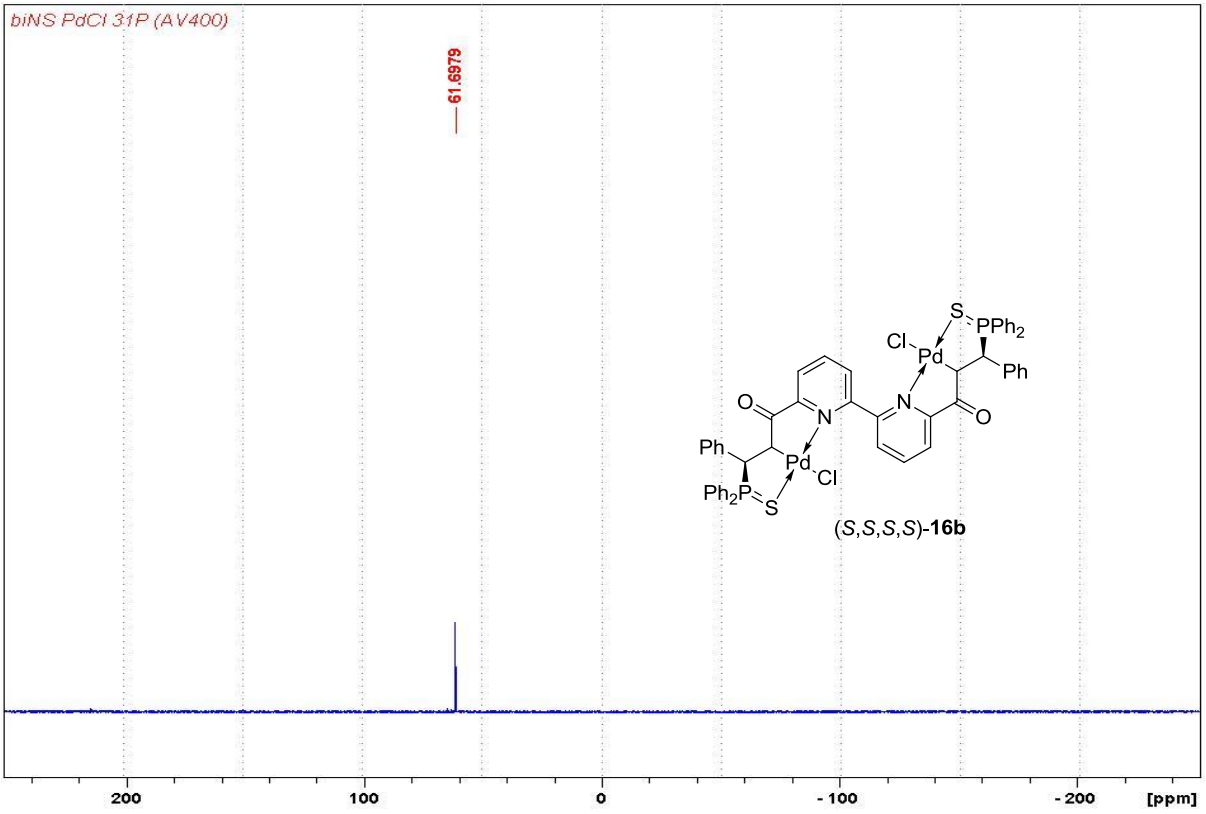

Figure s53. $^{31}P\{^{1}H\}$ NMR spectrum of complex (*S*,*S*,*S*,*S*)-**16b**.

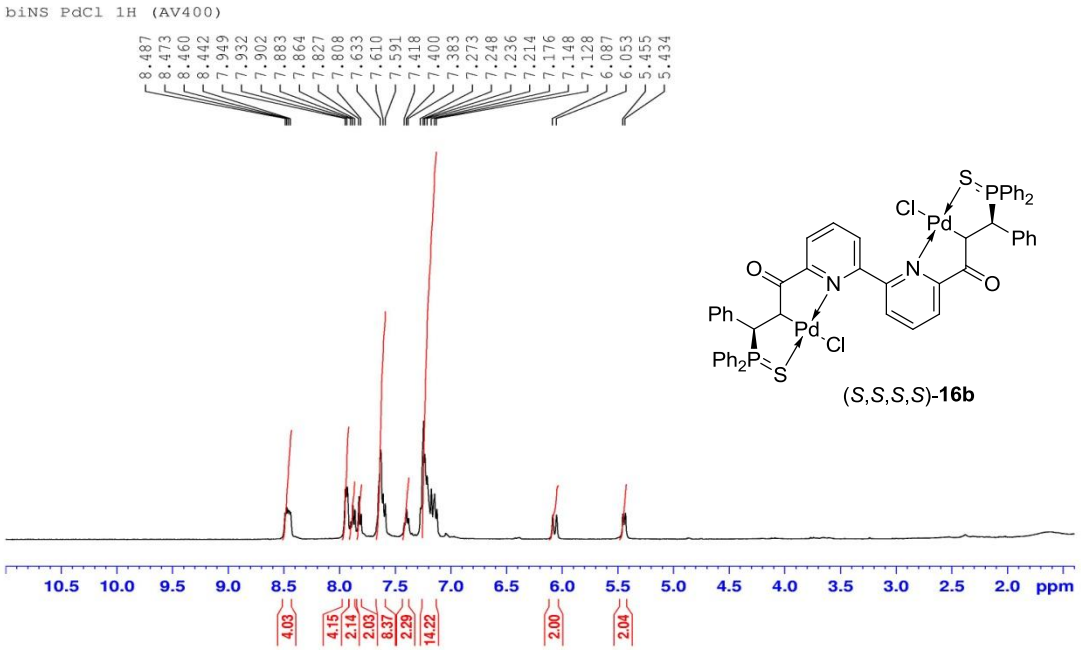

Figure s54. ^{1}H NMR spectrum of complex (*S*,*S*,*S*,*S*)-**16b**.

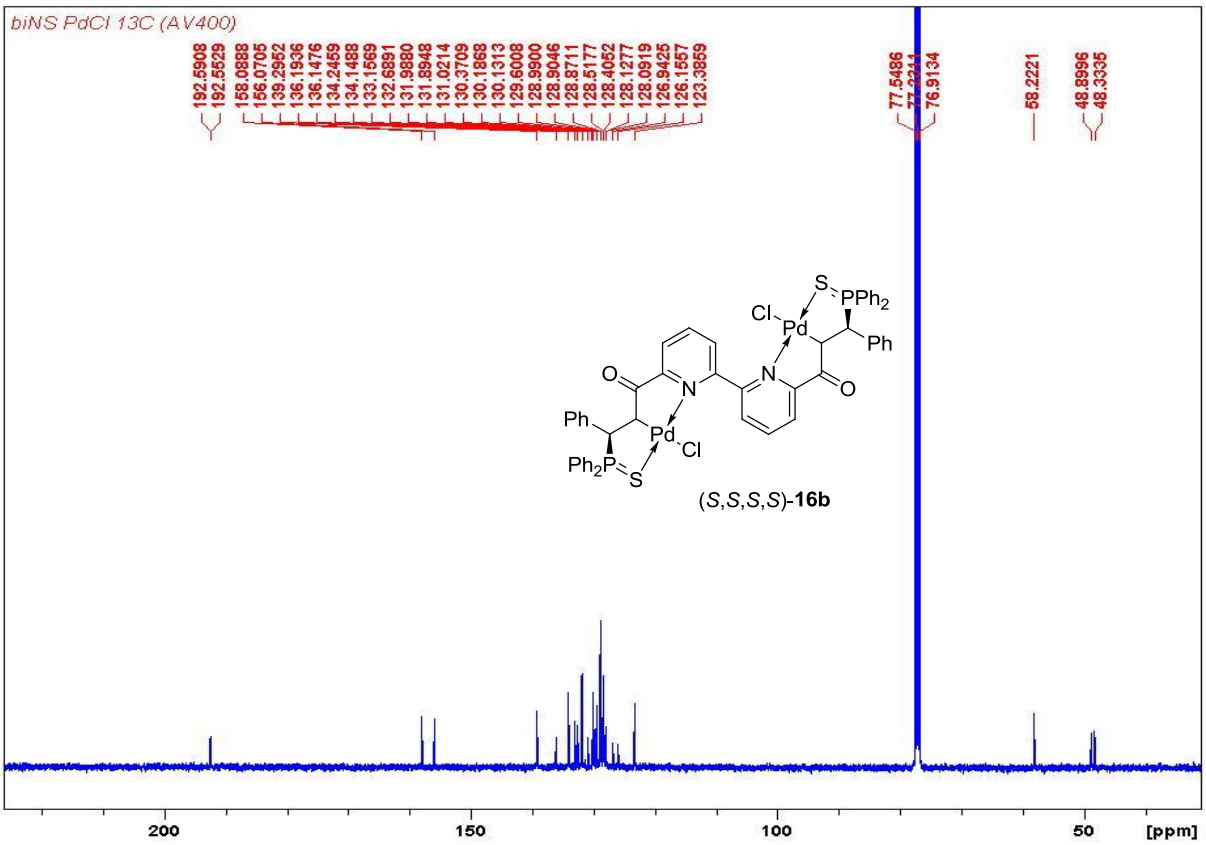

Figure s55. ^{13}C NMR spectrum of complex (*S*,*S*,*S*,*S*)-**16b**.

Determination of *ee*'s and *de*'s for bisphosphines 12 and 15

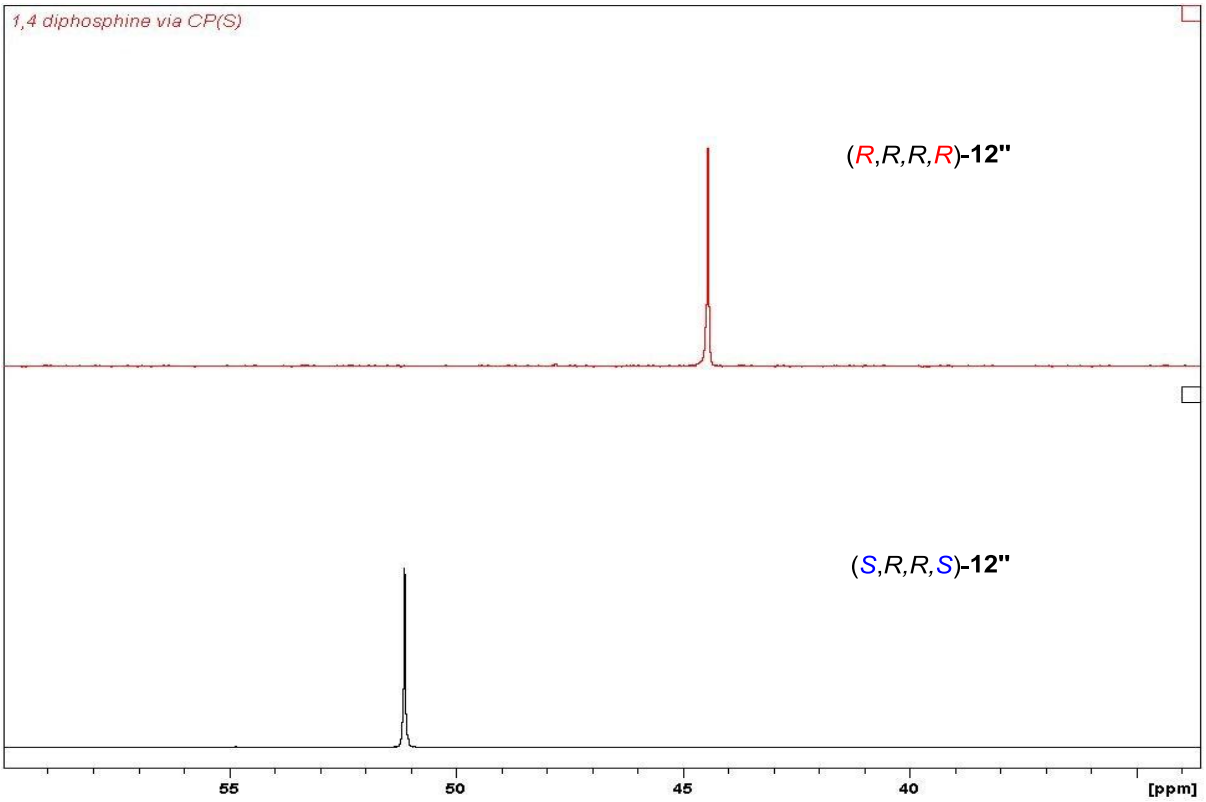

Figure s56. Determination of *ee* and *de* for bisphosphine **12'**.

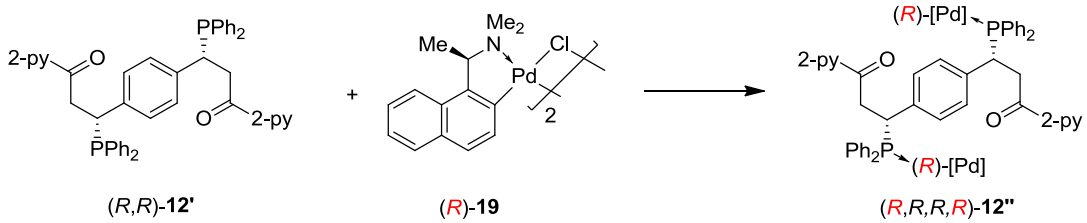

Scheme s2. Determination of *ee* and *de* for bisphosphine **12'**.

The determination of enantio- and diastereo-selectivity was conducted in a same manner as previously reported.[1] Theoretically, 3 isomers (*R*,*R*, *R*,*S*/*S*,*R* and *S*,*S*) may be formed *via* the double hydrophosphination reaction (in the case of a racemic mixture), and upon addition of a chiral derivatizing agent such as (*R*)-**19**, 3 phosphorous peaks corresponding to each diastereomers (*R*,*R*,*R*,*R*, *R*,*R*,*S*,*R*/*R*,*S*,*R*,*R*, and *R*,*S*,*S*,*R*) may be observed (in the case of a racemic mixture). A separate experiment involving the same crude reaction mixture but with the chiral derivatizing agent (*S*)-**19** serves as a confirmation of the results obtained. Since we only observed the appearance of one $^{31}P\{^{1}H\}$ NMR signal in each experiment, this indicates that the *ee* and *de* of bisphosphine **12'** (obtained from the hydrophosphination reaction) are >99%.

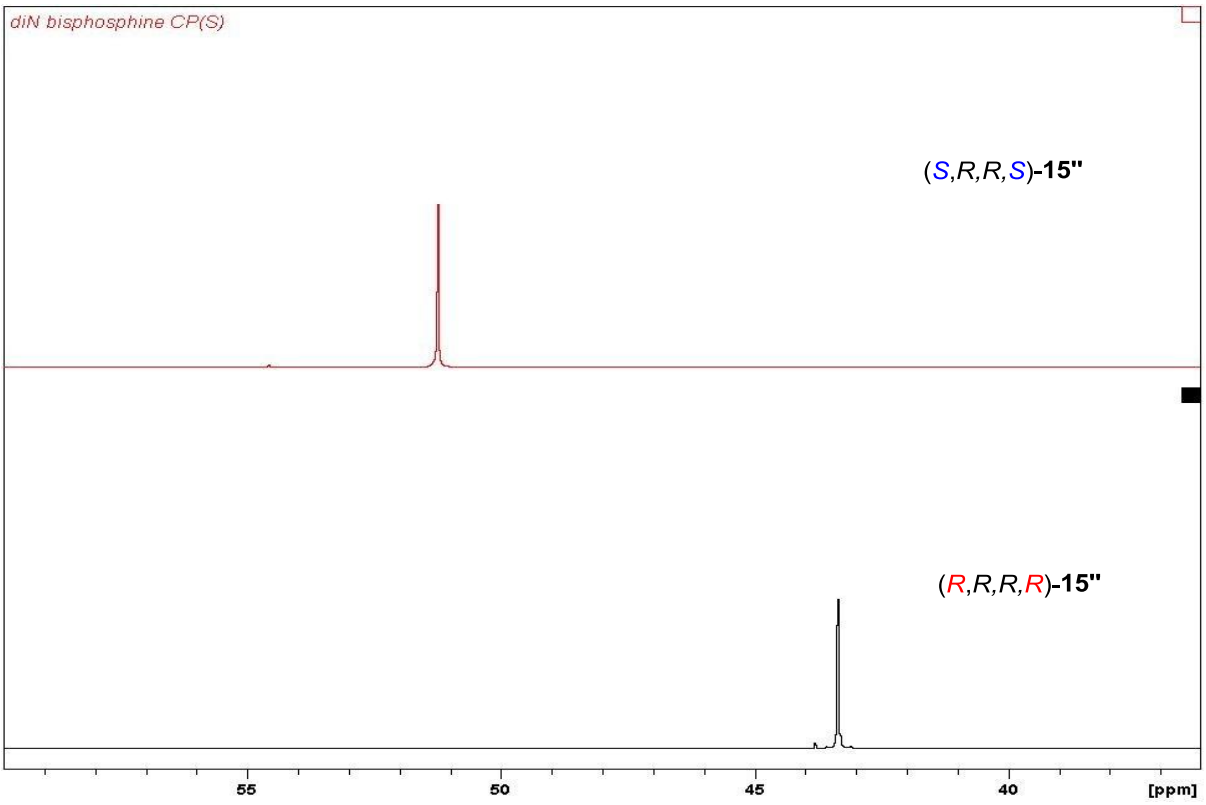

Figure s57. Determination of *ee* and *de* for bisphosphine **15'**.

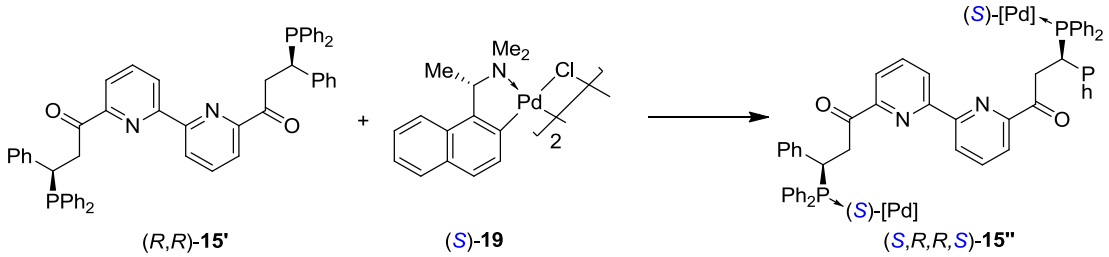

Scheme s3. Determination of *ee* and *de* for bisphosphine **15'**.

Similarly, employing the same technique as discussed above, 3 isomers (*R,R*, *R,S/S,R* and *S,S*) may be formed *via* the double hydrophosphination reaction (in the case of a racemic mixture). Upon addition of the chiral derivatizing agent (*S*)-**19**, 3 phosphorous peaks corresponding to each diastereomers (*S,R,R,S*, *S,R,S,S*/*S,S,R,S*, and *S,S,S,S*) may be observed (in the case of a racemic mixture). A separate experiment involving the same crude reaction mixture but with the chiral derivatizing agent (*R*)-**19** serves as a confirmation of the results obtained. Since we only observed the appearance of one $^{31}P\{^{1}H\}$ NMR signal in each experiment, this indicates that the *ee* and *de* of bisphosphine **15'** (obtained from the hydrophosphination reaction) are >99%.

Molecular Structures of NC(sp^3)S Pincer Complexes 4b and 9b

The X-ray crystal structures of both complexes (*S*,*S*)-**4b** and (*S*,*S*,*S*,*S*)-**9b** exhibited distorted square planar geometries about the Pd centers. Similar to the monomeric species (*S*,*S*)-**4b**, the stereogenic tertiary carbon centers in all the dimeric complexes generated from the asymmetric hydrophosphination adopted the (*S*)-absolute configuration. Likewise, all the chiral palladium-bound carbon centers in the current series of aliphatic pincer complexes adopted the (*S*)-absolute configurations. The selected bond lengths and angles of complexes (*S*,*S*)-**4b** and (*S*,*S*,*S*,*S*)-**9b** are collated in Table s1. Similar Pd←N [**4b**: 2.052(4) Å, **9b**: 2.047(4) Å] and Pd←S bond lengths [**4b**: 2.298(1) Å, **9b**: 2.292(1) Å] were observed in both complexes. A slightly longer Pd-C bond was recorded for complex **9b** [2.061(4) Å] than complex **4b** [2.045(5) Å] likely due to steric interactions between the two adjacent –PPh_2 motifs in **9b**. We believe that a more meaningful comparison of bond lengths could only be achieved after more EC(sp^3)E' Pd pincer complexes are reported in literature.

Table s1. Selected bond lengths (Å) and angles (°) of NC(sp^3)S pincer complexes **4b** and **9b**.

	(*S*,*S*)-**4b**	(*S*,*S*,*S*,*S*)-**9b**
Pd←N	2.052(4)	2.047(4)
Pd←S	2.298(1)	2.292(1)
Pd−Cl	2.396(1)	2.382(1)
Pd−C	2.045(5)	2.061(4)
C−Pd←S	90.89(15)	91.50(13)
C−Pd←N	82.21(19)	81.50(17)
C−Pd−Cl	174.72(15)	170.94(12)
Cl−Pd←S	92.94(5)	92.66(4)
Cl−Pd←N	94.04(13)	95.58(11)
N→Pd←S	172.93(13)	168.56(11)

HPLC Spectrum

```
Sample Info      : diethylcinnamylidenemalonate HP KOAc pyPCP PdCl RT DEE
                   24h
                   Eluant: 75H:25IPA 0.8mL/min
                   Column: AD-H 23C

Additional Info : Peak(s) manually integrated
```

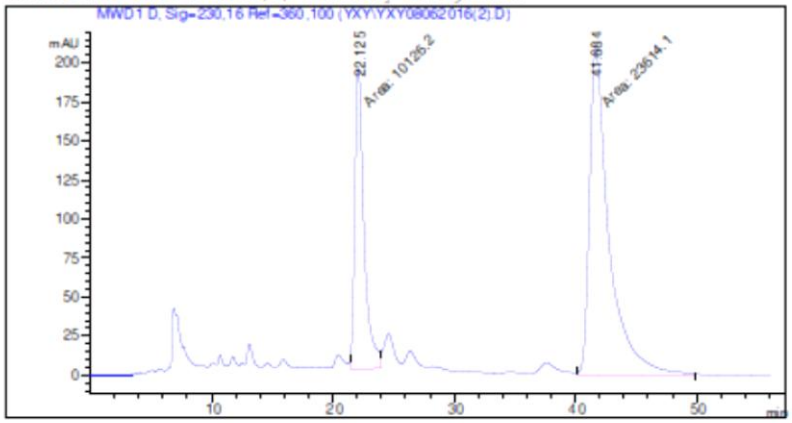


```
-------------------------------------------------------------------
                        Area Percent Report
-------------------------------------------------------------------

Sorted By             :      Signal
Multiplier:                   :      1.0000
Dilution:                     :      1.0000
Sample Amount:                :      1.00000  [ng/ul]    (not used in calc.)
Use Multiplier & Dilution Factor with ISTDs


Signal 1: MWD1 D, Sig=230,16 Ref=360,100

Peak RetTime Type  Width     Area      Height     Area
  #   [min]        [min]   [mAU*s]     [mAU]       %
----|-------|----|-------|---------|---------|-------|
   1  22.125 MF    0.8780 1.01262e4   192.22949  30.0121
   2  41.684 MM    1.8785 2.36141e4   209.51233  69.9879

Totals :                  3.37403e4   401.74182
```

Figure s58. HPLC Spectrum of compound **18b** in Table 1 Entry 9.

The signals associated with compound **18b** was verified with the HPLC data obtained in an earlier report.[6]

Crystallographic Data

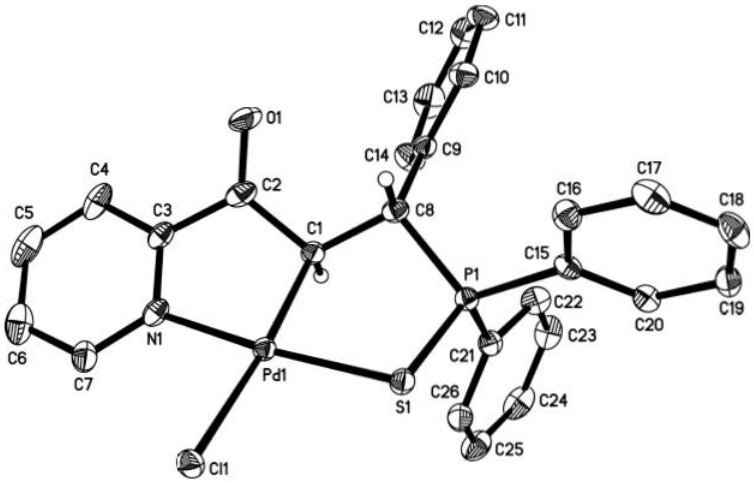

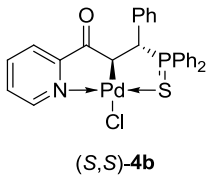

(*S*,*S*)-**4b**

Figure s59. ORTEP of NCS Pd pincer complex (*S*,*S*)-**4b**.

Table s2. Data collection and structure refinement for complex (*S*,*S*)-**4b**.

Chemical formula	$C_{27}H_{23}Cl_3NOPPdS$	
Formula weight	653.24 g/mol	
Temperature	103(2) K	
Wavelength	0.71073 Å	
Crystal size	0.100 x 0.120 x 0.420 mm	
Crystal habit	yellow block	
Crystal system	monoclinic	
Space group	P 1 21 1	
Unit cell dimensions	a = 9.7127(5) Å	α = 90°
	b = 11.5076(6) Å	β = 105.963(4)°
	c = 12.7323(6) Å	γ = 90°
Volume	1368.21(12) $Å^3$	
Z	2	
Density (calculated)	1.586 g/cm^3	
Absorption coefficient	1.127 mm^{-1}	
F(000)	656	
Theta range for data collection	3.44 to 35.13°	
Index ranges	-15<=h<=15, -18<=k<=18, -19<=l<=20	
Reflections collected	37087	
Independent reflections	12103 [R(int) = 0.0884]	
Coverage of independent reflections	99.5%	
Absorption correction	multi-scan	
Max. and min. transmission	0.8960 and 0.6490	
Refinement method	Full-matrix least-squares on F^2	
Refinement program	SHELXL-2014/6 (Sheldrick, 2014)	

Function minimized	$\Sigma\, w(F_o^2 - F_c^2)^2$	
Data / restraints / parameters	12103 / 1 / 316	
Goodness-of-fit on F^2	0.988	
Δ/σ_{max}	0.001	
Final R indices	9028 data; I>2σ(I)	R1 = 0.0543, wR2 = 0.0968
	all data	R1 = 0.0840, wR2 = 0.1103
Weighting scheme	$w=1/[\sigma^2(F_o^2)+(0.0362P)^2]$ where $P=(F_o^2+2F_c^2)/3$	
Absolute structure parameter	0.0(0)	
Largest diff. peak and hole	0.960 and -1.311 eÅ^{-3}	
R.M.S. deviation from mean	0.154 eÅ^{-3}	

Table s3. Bond lengths (Å) for complex (*S*,*S*)-**4b**.

Pd1-C1	2.045(5)	Pd1-N1	2.052(4)	C17-C18	1.388(9)
Pd1-S1	2.2976(13)	Pd1-Cl1	2.3963(12)	C19-C20	1.388(7)
C1-C2	1.499(8)	C1-C8	1.540(7)	C21-C22	1.404(8)
C2-O1	1.219(7)	C2-C3	1.487(8)	C22-C23	1.385(8)
C3-N1	1.348(7)	C3-C4	1.382(8)	C24-C25	1.377(9)
C4-C5	1.381(10)	C5-C6	1.387(9)	C27-Cl3	1.762(7)
C6-C7	1.383(8)	C7-N1	1.338(7)	P1-S1	2.0126(18)
C8-C9	1.513(7)	C8-P1	1.823(5)	C18-C19	1.385(8)
C9-C14	1.383(7)	C9-C10	1.401(8)	C21-C26	1.382(8)
C10-C11	1.392(7)	C11-C12	1.361(9)	C21-P1	1.808(6)
C12-C13	1.390(10)	C13-C14	1.388(8)	C23-C24	1.392(9)
C15-C20	1.394(7)	C15-C16	1.403(7)	C25-C26	1.398(8)
C15-P1	1.800(5)	C16-C17	1.383(7)	C27-Cl2	1.764(7)

Table s4. Bond angles (°) for complex (*S*,*S*)-**4b**.

C1-Pd1-N1	82.21(19)	C1-Pd1-S1	90.89(15)	C22-C21-P1	120.3(4)
N1-Pd1-S1	172.93(13)	C1-Pd1-Cl1	174.72(15)	C22-C23-C24	119.9(6)
N1-Pd1-Cl1	94.04(13)	S1-Pd1-Cl1	92.94(5)	C24-C25-C26	119.6(6)
C2-C1-C8	113.1(4)	C2-C1-Pd1	101.4(3)	Cl3-C27-Cl2	111.0(4)
C8-C1-Pd1	118.0(3)	O1-C2-C3	121.3(6)	C7-N1-Pd1	127.0(4)
O1-C2-C1	124.6(6)	C3-C2-C1	113.9(5)	C15-P1-C21	108.6(2)
N1-C3-C4	122.5(6)	N1-C3-C2	111.8(5)	C21-P1-C8	108.5(2)
C4-C3-C2	125.7(6)	C5-C4-C3	117.9(6)	C21-P1-S1	113.87(18)
C4-C5-C6	120.0(6)	C7-C6-C5	118.9(6)	P1-S1-Pd1	98.99(6)
N1-C7-C6	121.4(5)	C9-C8-C1	115.0(4)	C23-C22-C21	119.4(6)
C9-C8-P1	117.3(4)	C1-C8-P1	104.0(3)	C25-C24-C23	120.9(6)
C14-C9-C10	118.6(5)	C14-C9-C8	122.4(5)	C21-C26-C25	120.0(5)
C10-C9-C8	118.9(5)	C11-C10-C9	119.9(5)	C7-N1-C3	119.4(5)
C12-C11-C10	120.8(6)	C11-C12-C13	120.0(5)	C3-N1-Pd1	113.5(4)
C14-C13-C12	119.6(6)	C9-C14-C13	121.0(6)	C15-P1-C8	112.7(2)
C20-C15-C16	119.9(5)	C20-C15-P1	121.5(4)	C15-P1-S1	107.90(17)
C16-C15-P1	118.1(4)	C17-C16-C15	119.5(6)	C8-P1-S1	105.33(18)
C16-C17-C18	120.4(6)	C19-C18-C17	120.3(5)	C26-C21-C22	120.2(5)
C18-C19-C20	119.9(6)	C19-C20-C15	120.0(5)	C26-C21-P1	119.5(4)

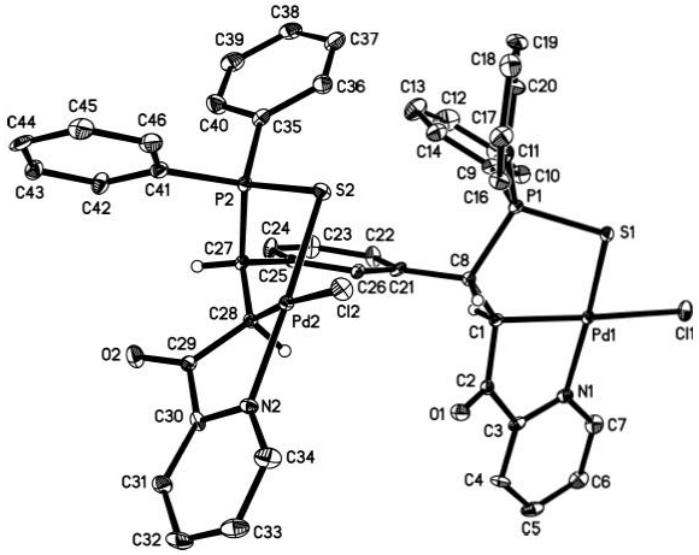

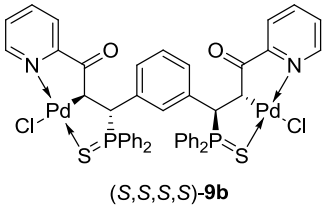

(*S*,*S*,*S*,*S*)-**9b**

Figure s60. ORTEP of NCS Pd pincer complex (*S*,*S*,*S*,*S*)-**9b**.

Table s5. Data collection and structure refinement for complex (*S*,*S*,*S*,*S*)-**9b**.

Chemical formula	$C_{49}H_{42}Cl_8N_2O_2P_2Pd_2S_2$	
Formula weight	1313.30 g/mol	
Temperature	103(2) K	
Wavelength	0.71073 Å	
Crystal size	0.120 x 0.300 x 0.420 mm	
Crystal habit	yellow block	
Crystal system	monoclinic	
Space group	P 1 21 1	
Unit cell dimensions	a = 9.4797(8) Å	α = 90°
	b = 28.175(2) Å	β = 104.9626(15)°
	c = 10.1153(9) Å	γ = 90°
Volume	2610.1(4) $Å^3$	
Z	2	
Density (calculated)	1.671 g/cm^3	
Absorption coefficient	1.281 mm^{-1}	
F(000)	1312	
Theta range for data collection	2.08 to 31.07°	
Index ranges	-13<=h<=11, -40<=k<=40, -14<=l<=14	
Reflections collected	25467	
Independent reflections	15305 [R(int) = 0.0343]	
Coverage of independent reflections	97.2%	
Absorption correction	multi-scan	
Max. and min. transmission	0.8610 and 0.6150	
Refinement method	Full-matrix least-squares on F^2	
Refinement program	SHELXL-2014/6 (Sheldrick, 2014)	
Function minimized	$\Sigma\ w(F_o^2 - F_c^2)^2$	

Data / restraints / parameters	15305 / 1 / 604	
Goodness-of-fit on F^2	1.043	
Δ/σ_{max}	0.001	
Final R indices	14485 data; I>2σ(I)	R1 = 0.0359, wR2 = 0.0770
	all data	R1 = 0.0386, wR2 = 0.0784
Weighting scheme	$w=1/[\sigma^2(F_o^2)+(0.0246P)^2+0.7498P]$ where $P=(F_o^2+2F_c^2)/3$	
Absolute structure parameter	-0.031(12)	
Largest diff. peak and hole	0.970 and -0.711 eÅ^{-3}	
R.M.S. deviation from mean	0.107 eÅ^{-3}	

Table s6. Bond lengths (Å) for complex (*S*,*S*,*S*,*S*)-**9b**.

Pd1-N1	2.047(4)	Pd1-C1	2.061(4)	C29-O2	1.214(5)
Pd1-S1	2.2919(12)	Pd1-Cl1	2.3821(11)	C30-N2	1.348(6)
Pd2-N2	2.054(4)	Pd2-C28	2.059(4)	C31-C32	1.384(7)
Pd2-S2	2.2937(13)	Pd2-Cl2	2.3750(11)	C33-C34	1.375(7)
C1-C2	1.474(7)	C1-C8	1.524(6)	C35-C40	1.395(6)
C2-O1	1.213(5)	C2-C3	1.510(6)	C35-P2	1.803(5)
C3-N1	1.352(6)	C3-C4	1.389(6)	C37-C38	1.391(7)
C4-C5	1.382(7)	C5-C6	1.387(8)	C39-C40	1.390(7)
C6-C7	1.387(8)	C7-N1	1.349(6)	C41-C42	1.403(6)
C8-C21	1.520(6)	C8-P1	1.827(5)	C42-C43	1.383(6)
C9-C14	1.396(6)	C9-C10	1.407(6)	C44-C45	1.386(8)
C9-P1	1.797(5)	C10-C11	1.377(7)	C47-Cl3	1.769(5)
C11-C12	1.389(8)	C12-C13	1.379(8)	C29-C30	1.522(6)
C13-C14	1.392(7)	C15-C16	1.392(6)	C30-C31	1.368(7)
C15-C20	1.395(7)	C15-P1	1.805(5)	C32-C33	1.396(8)
C16-C17	1.403(7)	C17-C18	1.377(8)	C34-N2	1.336(6)
C18-C19	1.398(7)	C19-C20	1.398(7)	C35-C36	1.405(7)
C21-C26	1.398(6)	C21-C22	1.401(6)	C36-C37	1.372(7)
C22-C23	1.385(6)	C23-C24	1.398(6)	C38-C39	1.386(8)
C24-C25	1.399(6)	C25-C26	1.400(6)	C41-C46	1.397(6)
C25-C27	1.512(6)	C27-C28	1.548(6)	C41-P2	1.807(4)
C27-P2	1.822(5)	C28-C29	1.478(6)	C43-C44	1.389(7)
C45-C46	1.385(7)	C47-Cl4	1.769(5)	P1-S1	2.0138(15)
C48-Cl6	1.768(6)	C48-Cl5	1.773(6)	P2-S2	2.0071(15)
C49-Cl7	1.752(6)	C49-Cl8	1.763(7)		

Table s7. Bond angles (°) for complex (*S*,*S*,*S*,*S*)-**9b**.

N1-Pd1-C1	81.50(17)	N1-Pd1-S1	168.56(11)	C36-C35-P2	120.2(3)
C1-Pd1-S1	91.50(13)	N1-Pd1-Cl1	95.58(11)	C36-C37-C38	120.6(5)
C1-Pd1-Cl1	170.94(12)	S1-Pd1-Cl1	92.66(4)	C38-C39-C40	120.2(5)
N2-Pd2-C28	80.83(17)	N2-Pd2-S2	172.44(11)	C46-C41-C42	118.8(4)
C28-Pd2-S2	91.61(13)	N2-Pd2-Cl2	97.03(11)	C42-C41-P2	121.0(3)
C28-Pd2-Cl2	174.45(12)	S2-Pd2-Cl2	90.52(4)	C42-C43-C44	120.6(5)
C2-C1-C8	113.9(4)	C2-C1-Pd1	101.1(3)	C46-C45-C44	120.3(5)

C8-C1-Pd1	120.9(3)	O1-C2-C1	125.8(4)	Cl3-C47-Cl4	111.1(3)
O1-C2-C3	121.3(4)	C1-C2-C3	112.8(4)	Cl7-C49-Cl8	112.0(3)
N1-C3-C4	122.6(4)	N1-C3-C2	112.9(4)	C7-N1-Pd1	128.7(3)
C4-C3-C2	124.4(4)	C5-C4-C3	119.1(5)	C34-N2-C30	118.7(4)
C4-C5-C6	118.1(5)	C7-C6-C5	120.6(4)	C30-N2-Pd2	113.1(3)
N1-C7-C6	121.0(5)	C21-C8-C1	114.7(4)	C9-P1-C8	107.9(2)
C21-C8-P1	115.0(3)	C1-C8-P1	105.3(3)	C9-P1-S1	113.43(16)
C14-C9-C10	120.0(4)	C14-C9-P1	119.3(3)	C8-P1-S1	106.20(14)
C10-C9-P1	120.4(3)	C11-C10-C9	119.2(4)	C35-P2-C27	109.2(2)
C10-C11-C12	120.9(5)	C13-C12-C11	119.9(5)	C35-P2-S2	110.47(17)
C12-C13-C14	120.4(5)	C13-C14-C9	119.5(5)	C27-P2-S2	107.75(14)
C16-C15-C20	120.5(4)	C16-C15-P1	119.4(4)	C37-C36-C35	120.0(5)
C20-C15-P1	119.4(3)	C15-C16-C17	118.8(5)	C39-C38-C37	119.8(5)
C18-C17-C16	120.9(5)	C17-C18-C19	120.4(5)	C39-C40-C35	120.0(5)
C18-C19-C20	119.3(5)	C15-C20-C19	120.1(5)	C46-C41-P2	120.2(4)
C26-C21-C22	119.1(4)	C26-C21-C8	120.5(4)	C43-C42-C41	120.1(4)
C22-C21-C8	120.4(4)	C23-C22-C21	120.8(4)	C45-C44-C43	119.6(4)
C22-C23-C24	119.6(4)	C23-C24-C25	120.9(4)	C45-C46-C41	120.5(5)
C24-C25-C26	118.7(4)	C24-C25-C27	119.1(4)	Cl6-C48-Cl5	111.5(3)
C26-C25-C27	122.2(4)	C21-C26-C25	121.0(4)	C7-N1-C3	118.5(4)
C25-C27-C28	115.2(3)	C25-C27-P2	111.2(3)	C3-N1-Pd1	111.8(3)
C28-C27-P2	105.5(3)	C29-C28-C27	115.1(3)	C34-N2-Pd2	128.1(3)
C29-C28-Pd2	103.2(3)	C27-C28-Pd2	120.6(3)	C9-P1-C15	108.5(2)
O2-C29-C28	126.4(4)	O2-C29-C30	121.2(4)	C15-P1-C8	112.4(2)
C28-C29-C30	112.4(4)	N2-C30-C31	122.8(4)	C15-P1-S1	108.52(15)
N2-C30-C29	112.8(4)	C31-C30-C29	124.3(4)	C35-P2-C41	108.7(2)
C30-C31-C32	118.9(5)	C31-C32-C33	118.3(5)	C41-P2-C27	108.1(2)
C34-C33-C32	119.5(5)	N2-C34-C33	121.8(5)	C41-P2-S2	112.51(15)
C40-C35-C36	119.4(4)	C40-C35-P2	120.2(4)	P1-S1-Pd1	96.75(6)
P2-S2-Pd2	92.61(6)				